



Manawatū-Whanganui Region Catchment Nutrient Models: Model Updates

Supporting Regional Land and Water
Management

August 2022

Prepared for:

Lizzie Daly
Science Manager

August 2022
Report No. 2022/EXT/1770
ISBN 978-1-99-000997-6

Prepared by:

Tim Cox
RMA Science Ltd

Tim Kerr, Ton Snelder, & Caroline Fraser
LWP Ltd

CONTACT 24 hr freephone 0508 800 80

Help@horizons.govt.nz

www.horizons.govt.nz

SERVICE CENTRES	Kairanga Cnr Rongotea and Kairanga-Bunnythorpe Roads Palmerston North	REGIONAL HOUSES	Palmerston North 11-15 Victoria Avenue	DEPOTS	Taihape 243 Wairanu Road Taihape
	Marton 19 Hammon Street		Whanganui 181 Guyton Street		Woodville 116 Vogel Street
	Taumarunui 34 Maata Street				

POSTAL ADDRESS Horizons Regional Council, Private Bag 11025, Manawatū Mail Centre,
Palmerston North 4442

F 06-952 2929

RMA Science
Good decisions, good science

Hamilton
New Zealand



Manawatū-Whanganui Region Catchment Nutrient Models: Model Updates

**Supporting Regional Land and Water
Management**

August 2022

Prepared By:

Tim Cox¹

Tim Kerr²

Ton Snelder²

Caroline Fraser²

1. RMA Science Ltd
2. LWP Ltd

For any information regarding this report please contact:

Ton Snelder

Phone: 0275758888

Email: ton@lwp.nz

LWP Ltd

PO Box 70

Lyttelton 8092

New Zealand

LWP Client Report Number: 2022-02

Report Date: August 2022

Quality Assurance Statement


Version	Reviewed By	
Final	Simon Harris	

Table of Contents

Executive Summary	vii
1 Introduction	8
2 Methods	9
2.1 Modelling software	9
2.2 Modelled basins and sub-catchments	10
2.3 Observed water quality site loads.....	15
2.4 Point source discharges.....	15
2.5 Land use and diffuse source nutrient export coefficients	17
2.5.1 Land use and typologies.....	17
2.5.2 Diffuse source nutrient export coefficients	20
2.6 Analysis of sediment erosion P	26
2.7 Model Calibration	27
3 Results and Discussion	30
3.1 Analysis of Sediment Erosion P	30
3.2 Model Calibration Results	31
4 Summary and conclusion	48
5 Acknowledgements	51
6 References	52
Appendix A Water quality site load calculations	54
Appendix B Analysis of Observed TP Loads and Sediment P Simulations at Water Quality Monitoring Sites	58
Figures	
Figure 1. Manawatū River basin model domain and sub-catchments.	11
Figure 2. Rangitīkei River basin model domain and sub-catchments.....	12
Figure 3. Whanganui River basin model domain and sub-catchments. Includes the Kai Iwi, Northern Lakes, Mōwhānau and Kaitoke Lakes catchments	13
Figure 4. Whangaehu River basin model domain and sub-catchments.	14
Figure 5. Land use map of the Manawatū-Whanganui region.....	18
Figure 6. Dairy land use in the region allocated to a Dairy type.	19
Figure 7. Production regions and slope classes used to assign non-dairy pastoral land uses to a type defined by the McDowell et al. (2021) Sheep & Beef typology.....	20
Figure 8. Total nitrogen diffuse source nutrient export coefficients.	24
Figure 9. Total phosphorous diffuse source nutrient export coefficients.....	25
Figure 10. Correlation of residual TP with TP yields estimated using SedNetNZ (upper panel) and mean catchment slope (lower panel).	31
Figure 11. Areal distribution of calibrated diffuse pathway attenuation coefficients for TN, Manawatū River basin.	38

Figure 12. Areal distribution of calibrated diffuse pathway attenuation coefficients for TP, Manawatū River basin.	38
Figure 13. Areal distribution of calibrated diffuse pathway attenuation coefficients for TN, Rangitīkei River basin.	39
Figure 14. Areal distribution of calibrated diffuse pathway attenuation coefficients for TP, Rangitīkei River basin.	39
Figure 15. Areal distribution of calibrated diffuse pathway attenuation coefficients for TN, Whanganui River basin.	40
Figure 16. Areal distribution of calibrated diffuse pathway attenuation coefficients for TP, Whanganui River basin.	40
Figure 17. Areal distribution of calibrated diffuse pathway attenuation coefficients for TN, Whangaehu River basin.	41
Figure 18. Areal distribution of calibrated diffuse pathway attenuation coefficients for TP, Whangaehu River basin.	41
Figure 19. Total nitrogen calibrated diffuse pathway attenuation coefficients for each sub-catchment.	42
Figure 20. Total phosphorus calibrated diffuse pathway attenuation coefficients for each sub-catchment.	43
Figure 21. Calibrated observed sediment erosion phosphorus (OSEP) sub-catchment yields ($\text{kg ha}^{-1} \text{ year}^{-1}$).	44
Figure 22. Summary of source load distributions for downstream sites in modelled river basins.	45
Figure 23. Summary of land use distributions for downstream sites in modelled river basins.	46

Tables

Table 1. High-level summary of each of the four water quality models.	10
Table 2 Summary of point source loads that were explicitly represented by the models.	16
Table 3. Diffuse source nutrient export coefficients look-up-table.	21
Table 4. Diffuse source nutrient export coefficients for dairy land use.	22
Table 5. Diffuse source nutrient export coefficients for non-dairy pastoral land use.	23
Table 6. Fitted coefficients for multiple variable linear regression model explaining the between calibration points variation in residual TP.	30
Table 7. Comparison of calibrated Manawatū River basin model TN concentrations and loads with measured values.	33
Table 8. Comparison of calibrated Manawatū River basin model TP concentrations and loads with measured values.	34
Table 9. Comparison of calibrated Rangitīkei River basin model TN concentrations and loads with measured values.	35
Table 10. Comparison of calibrated Rangitīkei River basin model TP concentrations and loads with measured values.	35
Table 11. Comparison of calibrated Whanganui River basin model TN concentrations and loads with measured values.	36
Table 12. Comparison of calibrated Whanganui River basin model TP concentrations and loads with measured values.	36
Table 13. Comparison of calibrated Whangaehu River basin model TN concentrations and loads with measured values.	37
Table 14. Comparison of calibrated Whangaehu River basin model TP concentrations and loads with measured values.	37

Table 15. Baseline model TN source load distributions for example model locations ..47
Table 16. *Baseline model TP source load distributions for example model locations...47*

List of Abbreviations and Acronyms

Abbreviation	Full Name	Description
FMU	Freshwater Management Unit	As per National Policy Statement (2014), “A water body, multiple water bodies or any part of a water body determined by the regional council as the appropriate spatial scale for setting freshwater objectives and limits and for freshwater accounting and management.”
SCAMP	Simplified Contaminant Allocation Modelling Platform	Catchment modelling software
TN	Total Nitrogen	Includes both dissolved and particulate forms of nitrogen
TP	Total Phosphorus	Includes both dissolved and particulate form of nitrogen
DEP	Diffuse Export Phosphorus	Phosphorus loss from land surfaces, via surface and sub-surface pathways that is included in model export coefficients and is subject to diffuse pathway attenuation by the model
PSP	Point Source Phosphorus	Phosphorus loads from point sources
SEP	Sediment Erosion Phosphorus	Phosphorus loss from land surfaces occurring from large scale erosion and that is not included in DEP
OSEP	Observable Sediment Erosion Phosphorus	The portion of SEP that is included in observed instream loads

Executive Summary

Catchment water quality models representing loads and concentrations of total nitrogen and total phosphorous were developed for four major river basins (in the context of SCAMP this is four areas that may be made up of multiple catchments that are not necessarily connected) in the Horizons Region: the Manawatū, the Rangitikei the Whanganui, and the Whangaehu. The entire region is encapsulated by the four models. The models use sub-catchment diffuse contaminant export and attenuation coefficients and point source load estimates to simulate the generation, transport, and downstream delivery of total nitrogen (TN) and total phosphorus (TP) loads throughout the network. The models were developed to support catchment water quality management and planning. It is anticipated that the models will be used to estimate loads and concentrations under a range of management scenarios.

The models were rigorously calibrated for both TN and TP, making best use of the available data to the extent practicable. A guiding principle of the calibration process was to trust, and prioritise, site specific measured data over calculated or modelled data that aren't based on site specific observations. At certain steps in the calibration process, subjective decisions were made, out of necessity and based on best professional judgement. These are clearly documented herein. Such subjectivity is common to many modelling studies and is unavoidable when data are not available to objectively quantify all model parameters. It is worth noting that this conundrum could not be resolved, or even improved, with a more complex catchment model.

Satisfactory calibration was achieved for all four basin models and for both TN and TP. For TN, downstream calibration targets were all achieved with sensible adjustments to upstream attenuation coefficients, within expected ranges. For TP, calibrated attenuation coefficients were generally lower than those derived for TN. For multiple calibration sites, additional supplemental load source terms were required to achieve an adequate calibration. Conceptually, these source terms are hypothesised as representing the phosphorus (P) associated with large-scale erosion events within a given catchment that are not well represented by the independently derived model export coefficients. More precisely, it is the portion of this type of load that is included in the instream load estimates but is not included in the export coefficients. Correlation analyses revealed statistically significant correlations between the quantified supplemental P source terms and multiple landscape erodibility surrogates, thereby providing support for this hypothesis. The conceptual framework that has been presented can serve as a template for future catchment modelling in New Zealand, including erosion-based P that may be independently predictable, at least on a relative scale, with measurable landscape characteristics. Further investigation into spatial or physiographic patterns and/or correlations associated with the attenuation coefficients, or the supplemental source terms, was beyond the scope of the current study.

Models are uncertain, and the uncertainty of the key model parameters is largely unavoidable because it results from uncertainty in the water quality site TN and TP measurements and estimated sub-catchment TN and TP loads. This uncertainty needs to be considered when using the models to make predictions of TN and TP loads and concentrations under different management scenarios. The estimated loads and concentrations in absolute terms should be regarded as less certain than the relative difference in loads and concentrations between locations and scenarios.

1 Introduction

Horizons Regional Council (HRC) require appropriate scientific information to support objective and limit setting in the Manawatū-Whanganui region as part of its process to develop a new regional water plan that implements the National Policy Statement – Freshwater Management (NPS-FM; NZ Government, 2020). An important component of that information is how loss of contaminants from land in the Manawatū-Whanganui region can be managed to achieve water quality objectives in freshwater and coastal receiving environments.

There are a wide range of potential management actions and limits that could help to achieve water quality objectives. Identifying which set of actions and limits is preferred requires analysis for at least two reasons. First, the impacts of actions and limits will not be evenly distributed across the region because land use and receiving environment sensitivity to contaminants is spatially variable. Second, there is environmentally mediated variation in both potential contaminant losses from land use and the processing of contaminants (attenuation) as they move through the drainage network. Because these two factors interact, the assessment of options requires iterative simulation modelling of the land-water systems being managed. The basis for such simulation is catchment water quality models. Catchment water quality models account for the relevant processes such as contaminant loss from land and attenuation as well as spatial variation in factors such as current and potential land use.

This report describes the development and calibration of catchment water quality models that simulate the production, transport and attenuation of two important nutrients: nitrogen and phosphorus, in the Manawatū-Whanganui region. These models can be combined with models describing receiving environment response to provide a basis for iterative simulation modelling of the land-water systems in the region. This report does not describe the use of the models to perform simulation modelling; this will be the subject of other studies and documentation.

Catchment water quality models were developed for the Manawatū-Whanganui region's four major river basins: the Manawatū (including the Horowhenua and Coastal Tararua catchments), the Rangitīkei, the Whanganui, and the Whangaehu (including the Turakina River catchment). The entire region is encapsulated by the four models. The models use sub-catchment export and attenuation coefficients to simulate the generation, transport, and downstream delivery of total nitrogen (TN) and total phosphorous (TP) loads throughout the region. The models are based on the total forms of nitrogen and phosphorus because they represent a mass balance of both constituents at the catchment scale. However, the forms of both nutrients varies both in space and time and in some circumstances the dissolved forms of nitrogen and phosphorus are of interest¹. Where necessary, estimates of the proportion of the total that is in a particular form can be estimated from the TN and TP loads and/or concentrations predicted by the models but these estimates are external to the models.

The models can be used to investigate the potential effects of nutrient discharge from land (diffuse source discharges) and point source discharges. The models can be used to assess the effectiveness and feasibility of various options throughout the region including different sets of mitigation measures and land management practices, applying different discharge standards to land and/or point sources and changing land use. The models were developed in a usable framework to allow for future application by a range of potential end users. In future

¹ The NPS-FM requires that councils define nutrient concentration criteria for rivers to achieve periphyton target attribute states (NZ Government, 2020). This requirement stipulates the criteria are defined in terms of the dissolved fractions of TN and TP; namely dissolved inorganic nitrogen (DIN) and dissolved reactive phosphorus (DRP).

use of the models, the primary input will be scenario assumptions about land use (diffuse) and point source (direct) nutrient loads, and the primary outputs will be loads and concentrations at reporting locations distributed throughout the river network.

2 Methods

2.1 Modelling software

The Horizons models were developed using RMA Science's (RMA) Simplified Contaminant Allocation and Modelling Platform (SCAMP) software. SCAMP is designed as a flexible, and usable, generalised modelling tool for simulating diffuse and point source contamination at a catchment scale.

SCAMP calculates the generation of a range of user-defined contaminants at a catchment scale and the fate and transport of the contaminants through the catchment's stream network. Contaminant sources are represented in the model as individual nodes, parcels, or sub-catchments, discharging to specific streams. Contaminant sources can be either diffuse (e.g., farms) or point (e.g., municipal discharges). Sources can be aggregated for lower resolution models, including to a sub-catchment scale (in the context of models in the Horizons region this is to water management sub-zone scale), or explicitly represented as individual property parcels for higher resolution models. Diffuse source contamination calculations follow the widely used "export coefficient" approach, with prescribed areal average mass loading rates ($\text{kg ha}^{-1} \text{ yr}^{-1}$) linked to land use categories. Point sources are represented as point nodes with loading rates (kg yr^{-1}) defined for each. Both diffuse and point source loading parameters can be prescribed as seasonally variable in SCAMP.

Four forms of contaminant attenuation are available in the model: diffuse pathway, instream, wetland, and reservoir. The first is applicable for diffuse sources only and represents potential mass losses occurring from the point of export, or leaching, to the point of discharge to the receiving stream. The second captures attenuation that may occur during downstream transport within the stream channel (e.g., due to settling, uptake, or transformation). The third allows for the simulation of wetland interception and attenuation, as a function of calculated hydraulic residence time. Similarly, the fourth form of attenuation in the model provides for additional enhanced attenuation that may occur in intercepting reservoirs or lakes as a function of residence time. Each form of attenuation requires a user-prescribed rate constant. Like the source terms described above, all attenuation parameters can be defined seasonally in the model.

Note that, for the Horizons models described here, only diffuse pathway attenuation is included. Both export coefficients and attenuation coefficients are prescribed on an average annual basis. Parameter seasonality is not included in the current models. All lakes and wetlands in the region are only implicitly included in the constructed models.

Any number of water quality "output stations" (which in this context of the Horizons models are the bottom of the water management sub-zones) can be defined in the model at any instream location. These model objects provide for output summaries specific to the given location. These summaries include total contaminant loads (kg/month), concentration (mg/L), and source tracking (a breakdown of contributing upstream sources). Instream target concentrations (i.e., water quality observations) at these sites can be used for reference or to guide model calibration exercises.

SCAMP offers three modes of simulation: deterministic, stochastic, and optimisation. Deterministic simulations involve the tracking of contaminant mass from point of export (diffuse) or discharge (point) through a stream network to a series of downstream monitoring sites. The model generates source loads, which can vary seasonally, combines loads at appropriate locations, and attenuates the loads based on user-defined parameters, providing for time-varying loads (and/or concentrations) at any location in the modelled catchment. The model also provides useful source tracking output, showing relative contributions of load from upstream categories of diffuse and point sources. Up to four (4) different user-defined contaminants can be simulated in a single model.

Stochastic simulations allow the user to perform a comprehensive uncertainty analysis for their constructed model and to frame model predictions in the form of highly useful probability distributions. Rather than single value outputs of modelled river concentrations, stochastic simulations present these outputs in terms of exceedance probabilities (or “risk”). For stochastic simulations, simple probability distributions can be defined for any combination of the following key model inputs: export coefficients, diffuse pathway attenuation coefficients, and instream attenuation coefficients. Optimisation simulations perform the same fate and transport calculations as in deterministic and stochastic simulations but also provide an optimal mitigation strategy to achieve prescribed downstream water quality concentration targets. Optimality is determined in the model based on user-defined mitigation cost tables associated with each source node (sub-catchment land use class or point source). Note that only the deterministic mode of simulation was within scope for the modelling described here for Horizons.

2.2 Modelled basins and sub-catchments

Each river basin model was subdivided into sub-catchments based on HRC’s Water Management Zones (WMZ; Table 1). Each WMZ is represented in one of the four models (Figures 1 – 4).

Table 1. High-level summary of each of the four water quality models.

Model characteristics	Manawatū River	Rangitīkei River	Whanganui River	Whangaehu River
Total drainage area (ha)	747,000	394,300	760,800	314,800
Number of sub-catchments*	67	17	32	20
Number of point sources*	22	8	2	6
Number of water quality site calibration points	24	11	11	13
Number of explicit tributaries	30	8	18	10

*Note that model outputs are provided at assessment points that are located at the bottom of all sub-catchments and at point sources.

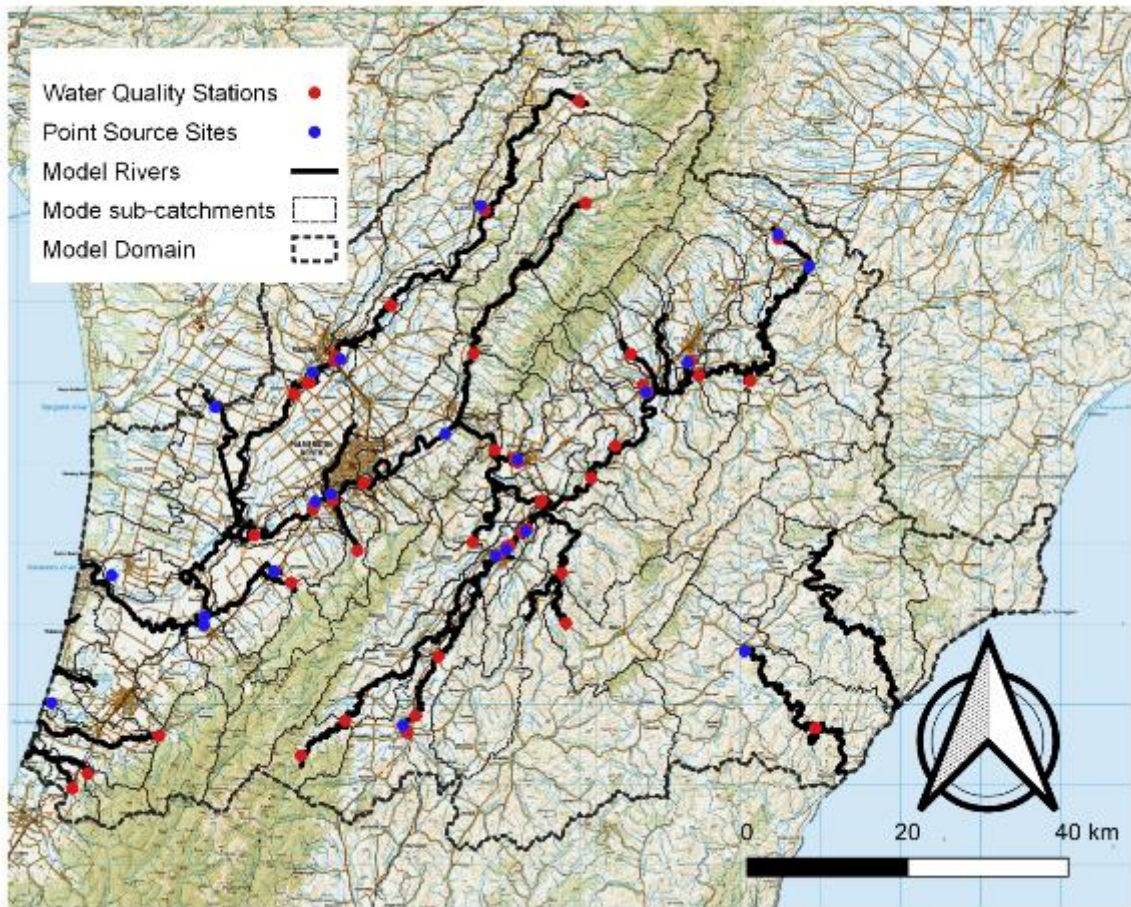


Figure 1. Manawātū River basin model domain and sub-catchments. Note that this model includes the Waiopehu and Puketoi ke tai catchments.

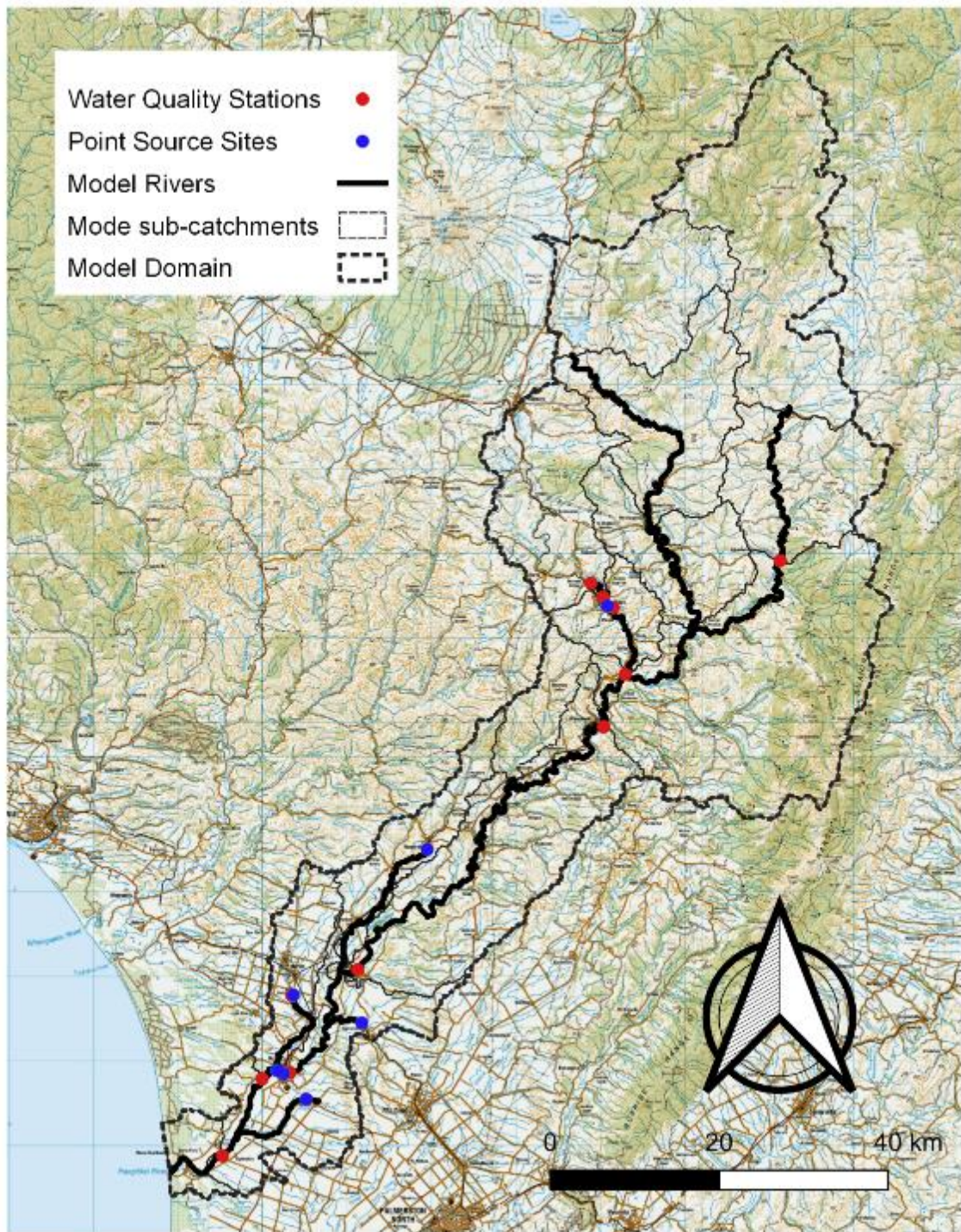


Figure 2. Rangitikei River basin model domain and sub-catchments.

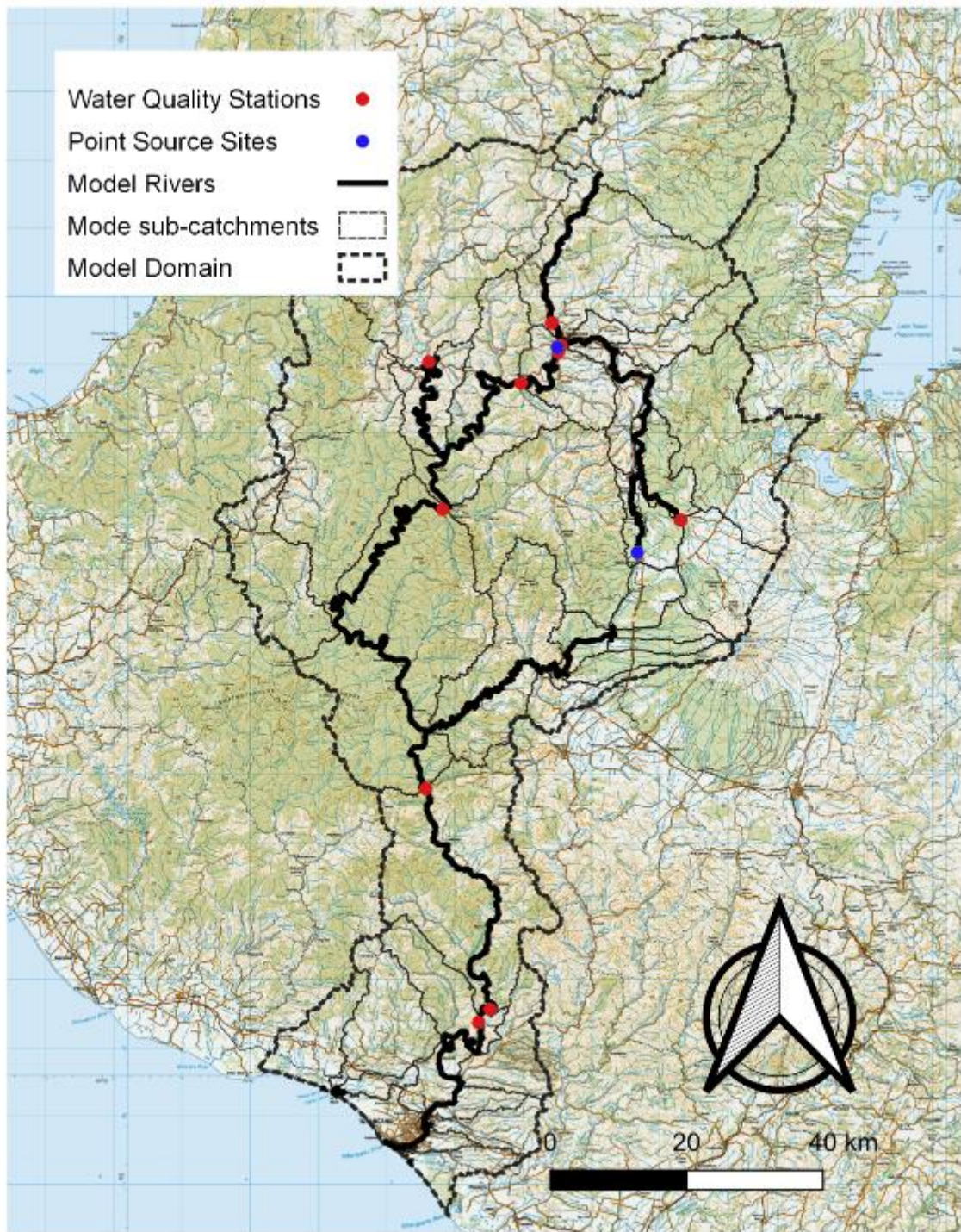


Figure 3. Whanganui River basin model domain and sub-catchments. Includes the Kai Iwi, Northern Lakes, Mōwhānau and Kaitoke Lakes catchments

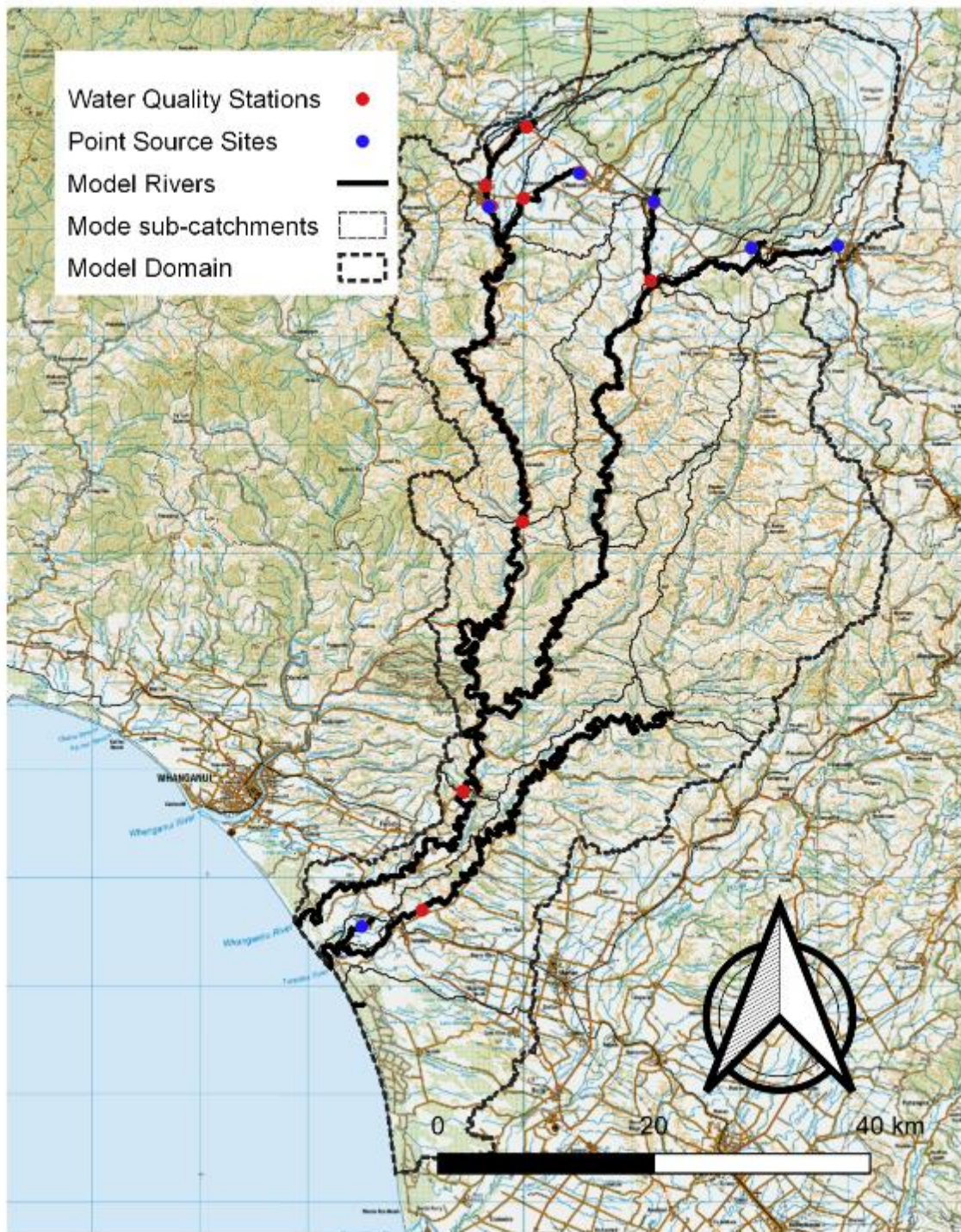


Figure 4. Whangaehu River basin model domain and sub-catchments. Note that this includes both the Whangaehu and Turakina Rivers and their catchments and the Southern Whanganui Lakes management zone.

2.3 Observed water quality site loads

Observations of mean annual loads of TN and TP at 55 water quality sites (locations shown in Figures 1 to 4) were calculated from monthly TN and TP concentrations and observed, or modelled, daily flows. The “observed” water quality site loads represent the loads of TN and TP that are observable from the monthly monitoring data. We assume that it is likely the observed loads under-estimate the total loads because monitoring is based on punctual monthly sampling that poorly characterises the TN and TP concentrations under infrequently occurring high-flow conditions. The observed loads were calculated to reflect catchment conditions in 2018 but based on long run average flow regime (i.e., the estimate is a mean annual load pertaining to catchment conditions in 2018). Details of the load calculation methods, including how the mean annual load pertaining to 2018 was evaluated, are provided in Appendix A and further details are contained in Fraser and Snelder (2020).

2.4 Point source discharges

Mean annual loads of TN and TP discharged at 38 industrial discharges and municipal wastewater treatment systems with consented discharges $>20\text{m}^3\text{d}^{-1}$ across the region were explicitly represented by the models. Data based on facility monitoring data describing discharge concentration of TN and TP for these point source discharges were provided by HRC. The point source loads were estimated for each discharge based on contaminant concentration monitoring data collected over the period from the start of 2014 to the end of 2018 as part of Horizons state of the environment monitoring programme. Discharge volume estimates were provided by HRC (mean daily flows, based on consented volumes, observed discharge rates and/or spot observations) from consent documents or compliance monitoring. Mean concentrations were calculated based on continuous or sporadic monitoring records for these discharges. The locations of the point source discharges are shown in Figure 1 to 4 and summarised in Table 2.

Some of the 38 discharges shown in Table 2 closed (i.e., were terminated) during the five-year period ending at the end of 2018. These closed discharges will nevertheless have influenced the estimates of the water quality site mean annual load pertaining to 2018 because the load estimation methods involve some temporal smoothing associated with the underlying regression models. We therefore included these closed discharges in the model calibration. However, we applied a reduction to the original load estimates for the closed discharges to reflect their closure. The reduction we applied to each of the closed discharges was equivalent to the proportion of the five-year period between 2014 and 2018 each discharge was in operation. For example, the Fonterra Pahiatua wastewater discharge closed near the end of 2014 and therefore the original load estimate was multiplied by approximately 1/5 to reflect the closure after year one of the five-year period.

Table 2 Summary of point source loads that were explicitly represented by the models.

Facility Name	River Basin	Modelled Receiving Stream	Estimated TN Load (kg y ⁻¹)	Estimated TP Load (kg y ⁻¹)	Closure date
AFFCO Fielding at Industrial	Manawatū	Ōroua River	41,155	11,309	
Ashhurst STP at Secondary	Manawatū	Manawatū River	308	128	09-06-2014
Dannevirke STP at	Manawatū	Mangatera Stream	65,778	14,244	
DB Breweries at Industrial	Manawatū	Mangatainoka River	136	44	28-07-2014
Eketāhuna STP at Secondary	Manawatū	Mākākahi River	1,847	276	
Feilding STP at Secondary	Manawatū	Ōroua River	314,252	912	
Fonterra Pahiatua wastewater	Manawatū	Mangatainoka River	45	2	30-11-2014
Foxton STP at Secondary	Manawatū	Manawatū	12,074	1,707	
Kimbolton STP at oxpond	Manawatū	Ōroua River	1,053	443	
Longburn STP at oxpond waste	Manawatū	Manawatū River	142	35	09-09-2014
Norsewood STP at oxpond	Manawatū	Manawatū River	684	214	
Ormondville STP at 2nd	Manawatū	Manawatū River	161	34	
Pahiatua STP at Tertiary	Manawatū	Mangatainoka River	3,238	580	
PNCC STP at tertiary treated	Manawatū	Manawatū River	438,398	37,534	
PPCS Oringi STP at oxpond	Manawatū	Ōruakeretaki Stream	306	7	
PPCS Shannon at clarifier	Manawatū	Manawatū River	165	88	13-03-2014
Rongotea STP at Secondary	Manawatū	Ōroua River	2,592	862	
Shannon STP at oxpond waste	Manawatū	Manawatū River	9,971	2,434	20-03-2017
Tokomaru at oxpond waste	Manawatū	Tokomaru River	241	42	
Woodville STP at Secondary	Manawatū	Mangaatua Stream	6,195	986	
Pongaroa STP at 2nd oxpond	Manawatū	Owahanga River	384	87	
The POT Levin STP	Manawatū	Waiwiri Stream	58,984	8,470	
Bulls STP at Secondary oxpond	Rangitīkei	Rangitīkei River	19,290	6,327	
Halcombe at Secondary	Rangitīkei	Rangitawa Stream	905	231	
Huntermville STP at	Rangitīkei	Pōrewa Stream	291	10	
Marton STP at Rock filtered	Rangitīkei	Tūtaenui Stream	26,889	5,419	
Ohakea STP at Effluent outfall	Rangitīkei	Rangitīkei River	19,290	6,327	
Riverlands at Industrial	Rangitīkei	Rangitīkei River	19,290	6,327	
Sanson STP at Secondary	Rangitīkei	Makowhai Stream	4,469	889	
Taihape STP at oxpond waste	Rangitīkei	Hautapu River	4,676	955	
National Park STP at	Whanganui	Piopiotea Stream	936	134	
Taumarunui STP at Tertiary treated waste	Whanganui	Whanganui River	15,261	3,042	
Ohakune STP at Secondary oxpond waste	Whangaehu	Mangawhero River	28,508	5,009	
Raetihi STP at Secondary oxpond waste	Whangaehu	Makotuku River	3,359	525	
Rangataua STP at Secondary	Whangaehu	Mangaehuehu Stream	188	36	
Waiouru STP at oxpond waste	Whangaehu	Waitangi Stream	6,529	1,216	
Winstone Pulp WWTP at	Whangaehu	Whangaehu River	26,812	4,764	
Ratana STP at Secondary	Whangaehu	Lake Waipu trib	584	91	

2.5 Land use and diffuse source nutrient export coefficients

The primary data inputs to SCAMP model for diffuse sources are the areas of land use in different categories in each sub-catchment and the associated estimates of diffuse source nutrient export coefficients. These data were converted to SCAMP input data for each model sub-catchment.

The diffuse source nutrient export coefficients were primarily provided by McDowell *et al.* (2021). McDowell *et al.* (2021) provide diffuse source nutrient export coefficients for pastoral land use in two land use categories: Dairy and Sheep & Beef. McDowell *et al.* (2021) uses “typologies” to provide for differences in export coefficients under each land use that are associated with variation in environmental factors. Separate typologies apply to Dairy and Sheep and Beef. Types within each typology are defined by categorical subdivision of the environmental factors climate, slope, drainage, and moisture, either explicitly (Dairy) or based partly on the use of production regions (i.e., geographic regions) to define the types (Sheep and Beef).

2.5.1 Land use and typologies

The main source of land use data was the primary classes (CLS_001) from the 2020 land use classification of Herzig *et al.* (2020), hereafter called Horizons land use map (Figure 5). For the purposes of determining diffuse source nutrient export coefficients, the pastoral land uses defined by the Horizons land use map (“Dairy farming”, “Sheep, beef, and/or deer farming”, “Other animal farming” and “Lifestyle”) were assigned to a type defined by McDowell *et al.* (2021) typologies. This process was complicated because the location of types defined by McDowell *et al.* (2021) typologies are not able to be mapped using publicly-available data. In addition, the available spatial data describing McDowell *et al.* (2021) typologies were already intersected with data describing the land use. A further complication was that polygons identified as pastoral land use on the Horizons land use map did not match perfectly with the land uses defined by McDowell *et al.* (2021) spatial data.

To obtain diffuse source nutrient export coefficients to polygons identified as “Dairy farming” on the Horizons land use map (hereafter “Dairy farming polygon”) we had to assign them to a type defined by the McDowell *et al.* (2021) Dairy typology (hereafter “Dairy type”). This assignment process was achieved in four steps. First, we spatially intersected the Dairy farming polygon defined by the Horizons land use map with the Dairy type polygons defined by the McDowell *et al.*'s (2021) typology. The Dairy farming polygons were assigned to the Dairy types they were intersected by. Second, where a Dairy farming polygon was intersected by more than one Dairy type polygon, the Dairy farming polygon was assigned to the Dairy type from the polygon with the greatest overlap. Third, where the Dairy farming polygon was not intersected by any Dairy type polygon, the Dairy farming polygons were assigned to the nearest Dairy type polygon within 100 m. Fourth, for 77 out of 1527 Dairy farming polygons there was no Dairy type polygon within 100 m. These 77 Dairy farming polygons were manually assigned to a Dairy type based on visual inspection of the spatial data. At the end of this process, all polygons defined as Dairy farming on the Horizons land use map were assigned to a Dairy type defined by the McDowell *et al.* (2021). The map of Dairy farming polygons and their assigned Dairy type is shown in Figure 6.

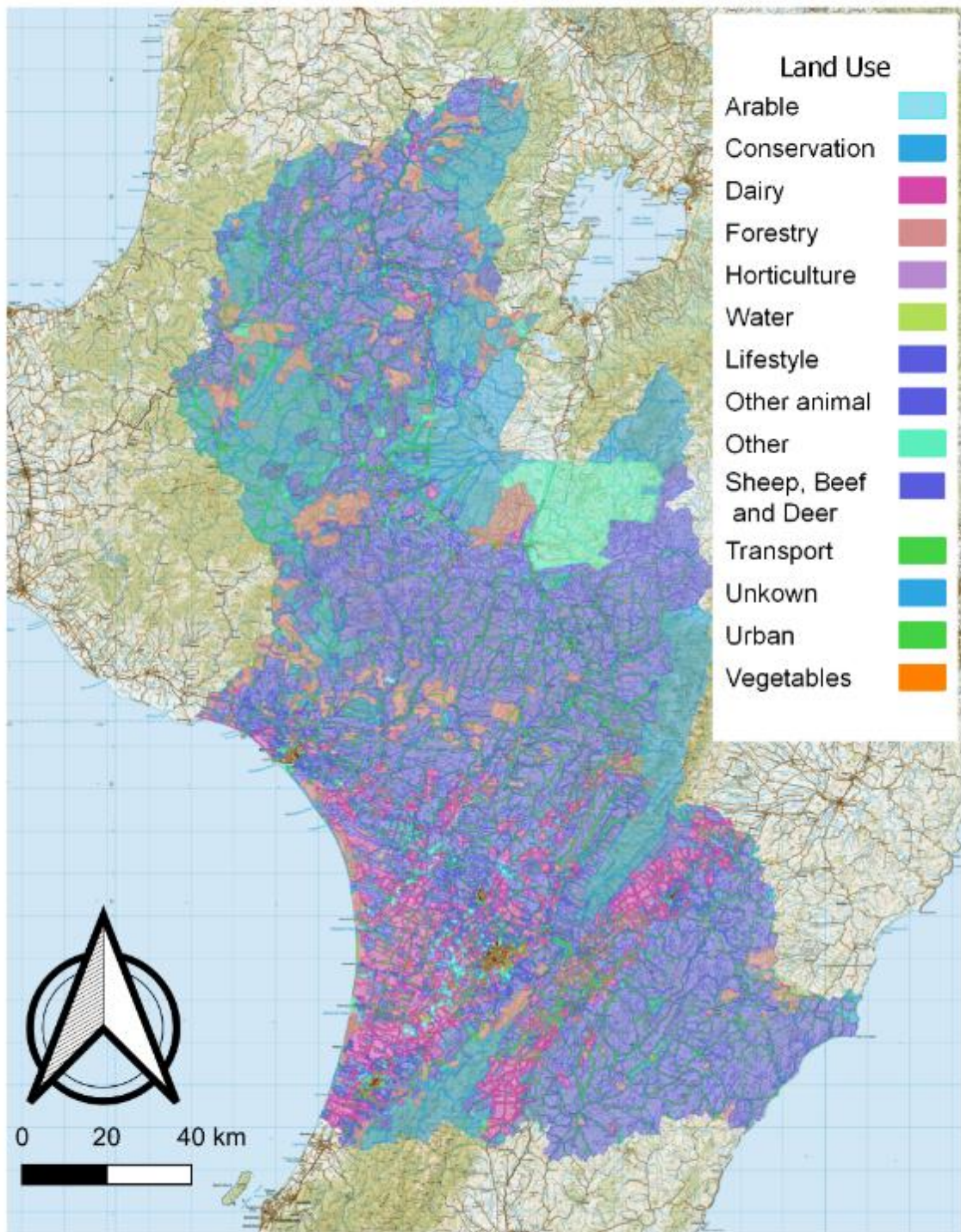


Figure 5. Land use map of the Manawatū-Whanganui region. From Herzig et al. (2021) CLS_001 primary land use class.

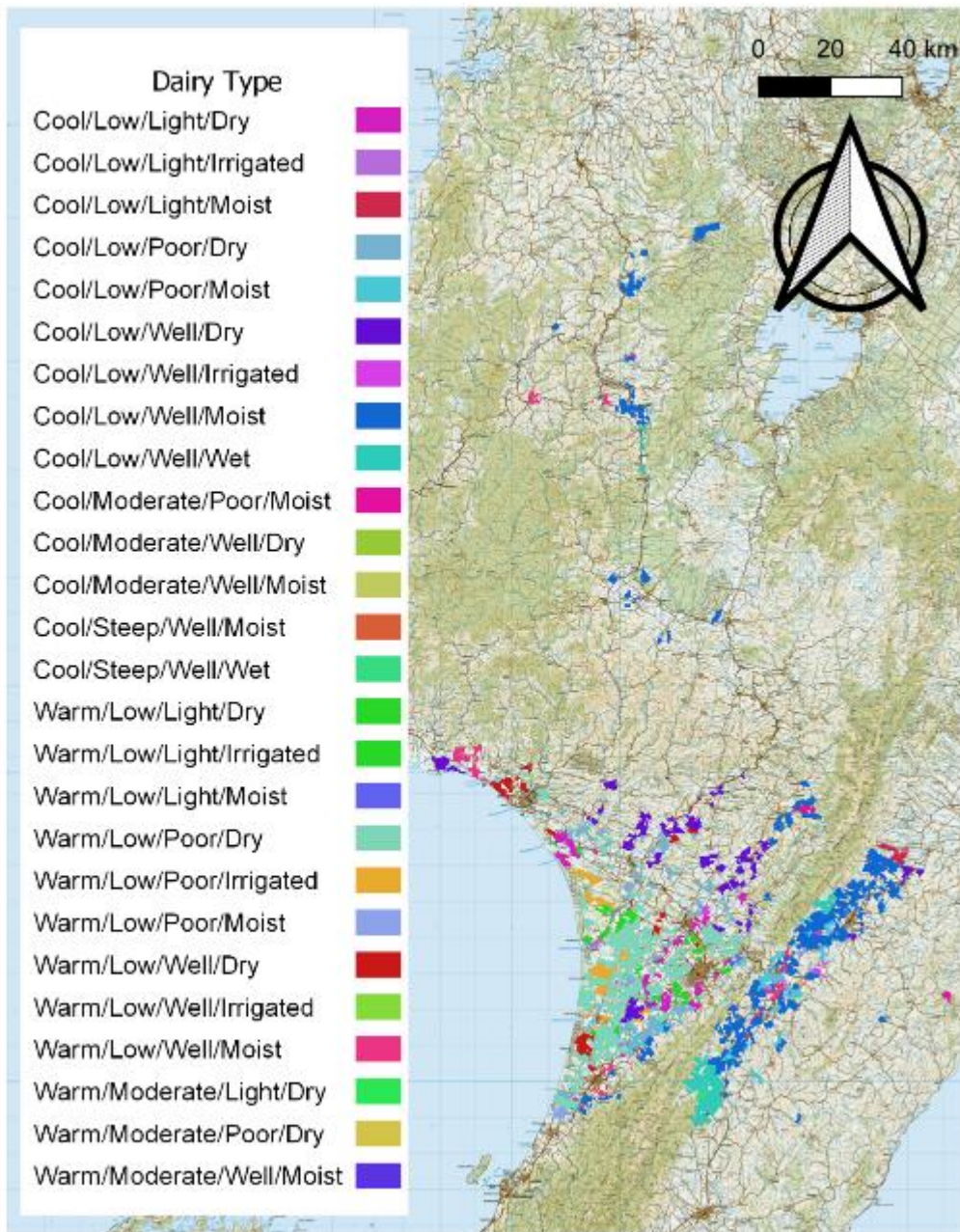


Figure 6. Dairy land use in the region allocated to a Dairy type. The Dairy type names are categories of climate, slope, drainage and moisture that are defined by the McDowell et al. (2021) Dairy typology.

To obtain diffuse source nutrient export coefficients for polygons identified as “Sheep, beef, and/or deer farming”, “Other animal farming” and “Lifestyle” (hereafter non-dairy pastoral land use) on the Horizons land use map we had to assign them to a type defined by the McDowell

et al. (2021) Sheep & Beef typology² (hereafter “Sheep & Beef type”). This assignment process was achieved in four steps.

First, we identified Sheep & Beef type polygons in McDowell *et al.*'s (2021) typology that belonged to each of the three Beef and Lamb NZ production regions that are represented in the Manawatū-Whanganui region: East Coast; Northland-Bay of Plenty-Waikato; Taranaki-Manawatū. Second, we merged the polygons assigned to each production region and defined non-intersecting convex hulls that enclosed each region, thereby creating a spatial layer that represented the three production regions within the Manawatū-Whanganui region (Figure 7). At the third step we subdivided the entire Manawatū-Whanganui into slope categories using spatial data provided by the New Zealand Land Resource Inventory “Slope” class (Newsome et al. 2008) and following the categories described in Monaghan et al. (2021) (Figure 7). At the fourth step, all polygons identified as non-dairy pastoral on the Horizons land use map were assigned to a Sheep & Beef type by intersecting them with the production region and slope layers (Figure 7).

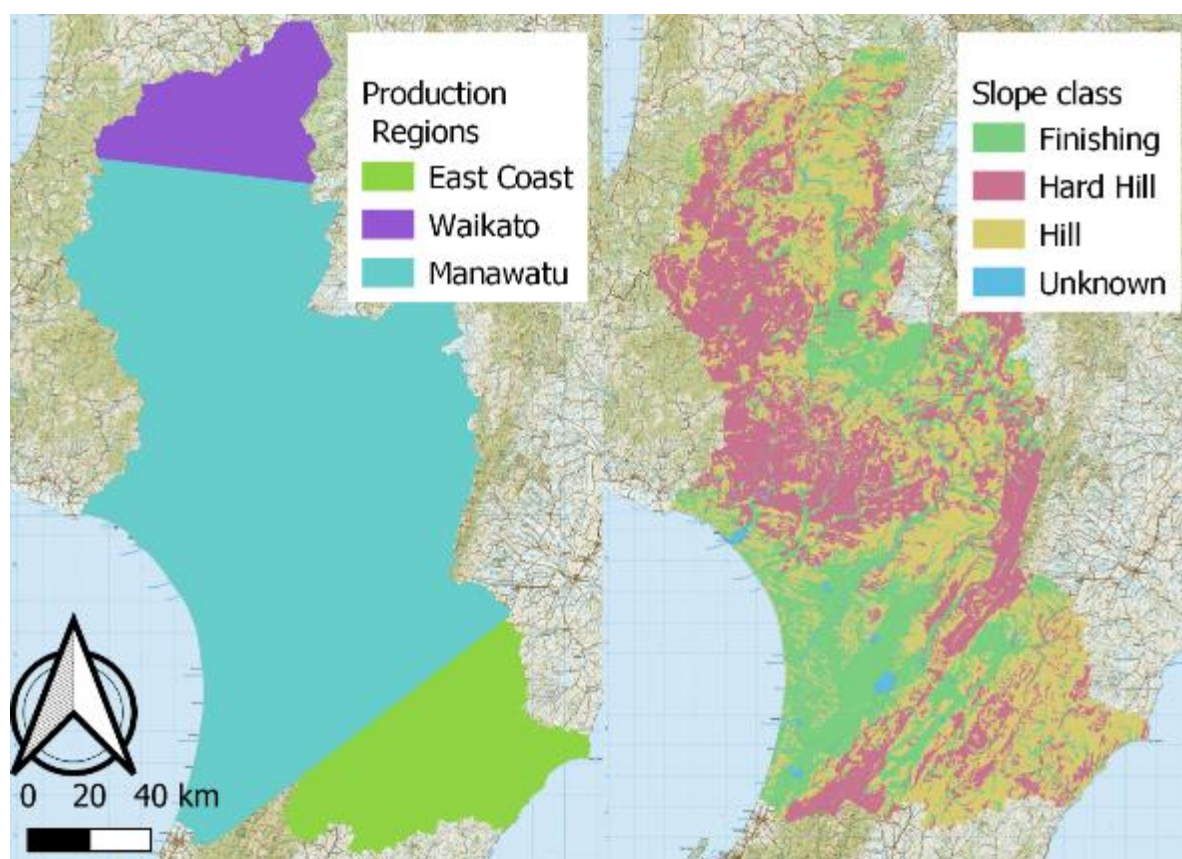


Figure 7. Production regions and slope classes used to assign non-dairy pastoral land uses to a type defined by the McDowell et al. (2021) Sheep & Beef typology.

2.5.2 Diffuse source nutrient export coefficients

Diffuse source nutrient export coefficients for all land in a pastoral farm land use were obtained by looking up their assigned Dairy type or Sheep & Beef type in the tables provided by McDowell *et al.* (2021) and obtaining the associated nutrient export coefficient or were based on an equivalent land use type defined by McDowell et al. (2021) following advice from Ross

² McDowell et al.'s (2021) Sheep & Beef types combine Beef and Lamb NZ production regions with slope classes.

Monaghan (AgResearch). Diffuse source nutrient export coefficients for the remaining land uses were based on literature values. Table 3 provides the diffuse loads and literature citation for the non-pastoral land use classes. Table 4 provides the diffuse loads for the dairy land use types and whether the values come direct from McDowell et al. (2021) or are based on an equivalent land use type. Table 5 provides the diffuse loads for the non-dairy pastoral land use types as defined in McDowell et al. (2021).

Table 3. Diffuse source nutrient export coefficients look-up-table.

Herzig (2020) Cls_001 Class	Description	Total Nitrogen Loss Rate (kg/Ha/Year)	Total Phosphorous Loss Rate (kg/Ha/Year)	Reference
URB	Urban	11	1.1	Moore et al. (2017)
VEG	Vegetable cropping	71	1.6	Bloomer et al. (2020)
DAI	Dairy	See Table 4		McDowell et al. (2021)
LIF	Lifestyle	See Table 5		As per SBD
HORT	Horticulture (other than VEG)	30	0.3	Drewry (2018)
ARA	Arable	30	0.3	Drewry (2018)
SBD	Sheep, beef, and/or deer	See Table 5		McDowell et al. (2021)
OAN	Other animal farming	See Table 5		As per SBD
FOR	Forestry	1.8	0.08	Drewry (2018)
CON	Conservation and amenity	1.6	0.33	Drewry (2018)
HYDR	Hydro parcels	0	0	
TRAN	Transport corridors	11	1.1	As per URB
OTH	Other	1.6	0.33	As per CON
UKN	Unknown	1.6	0.33	As per CON

Table 4. Diffuse source nutrient export coefficients for dairy land use.

Climate	Slope	Drainage	Moisture	Total Nitrogen Loss Rate (kg/Ha/Year)	Total Phosphorous Loss Rate (kg/Ha/Year)	Reference
Cool	Low	Light	Dry	43	0.6	As per warm equivalent
Cool	Low	Light	Irrigated	64	0.6	McDowell et al. 2021
Cool	Low	Light	Moist	60	0.6	As per warm equivalent
Cool	Low	Poor	Dry	26	0.6	McDowell et al. 2021
Cool	Low	Poor	Moist	37	1.2	McDowell et al. 2021
Cool	Low	Well	Dry	24	0.8	As per warm equivalent
Cool	Low	Well	Irrigated	113	2	McDowell et al. 2021
Cool	Low	Well	Moist	38	0.7	McDowell et al. 2021
Cool	Low	Well	Wet	60	0.7	McDowell et al. 2021
Cool	Moderate	Poor	Moist	27	4.5	As per warm equivalent
Cool	Moderate	Well	Dry	24	0.8	As per warm and low equivalent
Cool	Moderate	Well	Moist	36	1.8	As per warm equivalent
Cool	Steep	Well	Moist	36	1.8	As per moderate and warm equivalent
Cool	Steep	Well	Wet	44	6.6	As per moderate equivalent
Warm	Low	Well	Dry	43	0.6	McDowell et al. 2021
Warm	Low	Light	Irrigated	64	0.6	As per cool equivalent
Warm	Low	Light	Moist	60	0.6	Monaghan pers. Comms.
Warm	Low	Poor	Dry	26	1.5	McDowell et al. 2021
Warm	Low	Poor	Irrigated	46	0.9	As per cool equivalent
Warm	Warm	Poor	Moist	29	1.4	McDowell et al. 2021
Warm	Low	Well	Dry	24	0.8	McDowell et al. 2021
Warm	Low	Well	Irrigated	113	2	As per cool equivalent
Warm	Low	Well	Moist	34	1.2	Monaghan pers. Comms.
Warm	Moderate	Light	Dry	43	0.6	As per low equivalent
Warm	Moderate	Poor	Dry	27	0.8	As per cool equivalent
Warm	Moderate	Well	Moist	36	1.8	McDowell et al. 2021

Table 5. Diffuse source nutrient export coefficients for non-dairy pastoral land use. From McDowell et al. (2021).

Farming region	Slope	Total Nitrogen Loss Rate (kg/Ha/Year)	Total Phosphorous Loss Rate (kg/Ha/Year)
East Coast	Hard Hill	14	2
East Coast	Hill	17	1.5
East Coast	Finishing	30	1.2
Northland-Waikato-Bay of Plenty	Hard Hill	17	1.1
Northland-Waikato-Bay of Plenty	Hill	17	1.1
Northland-Waikato-Bay of Plenty	Finishing	21	4.6
Taranaki-Manawatū	Hard Hill	13	1
Taranaki-Manawatū	Hill	14	0.8
Taranaki-Manawatū	Finishing	16	1.1

Allocation of the diffuse source nutrient export coefficients to the land use data was applied on a 250 m x 250 m grid resulting in maps of diffuse loads for the Manawatū-Whanganui region (Figure 8 and Figure 9). The mean value of the diffuse source nutrient export coefficients was determined for each combination of SCAMP model sub-catchment, nutrient type (total nitrogen and total phosphorous) and Horizons land use class (Table 3).

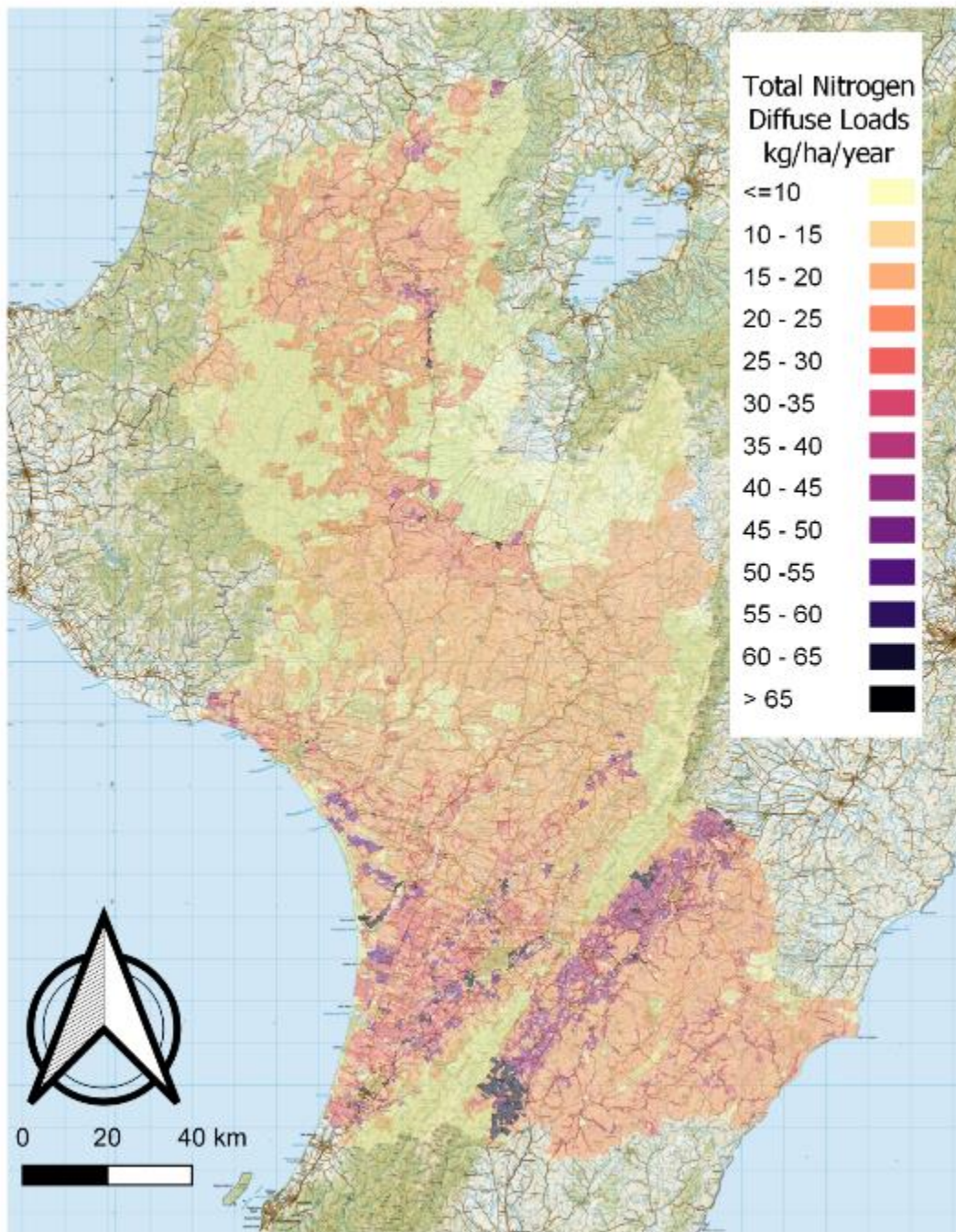


Figure 8. Total nitrogen diffuse source nutrient export coefficients.

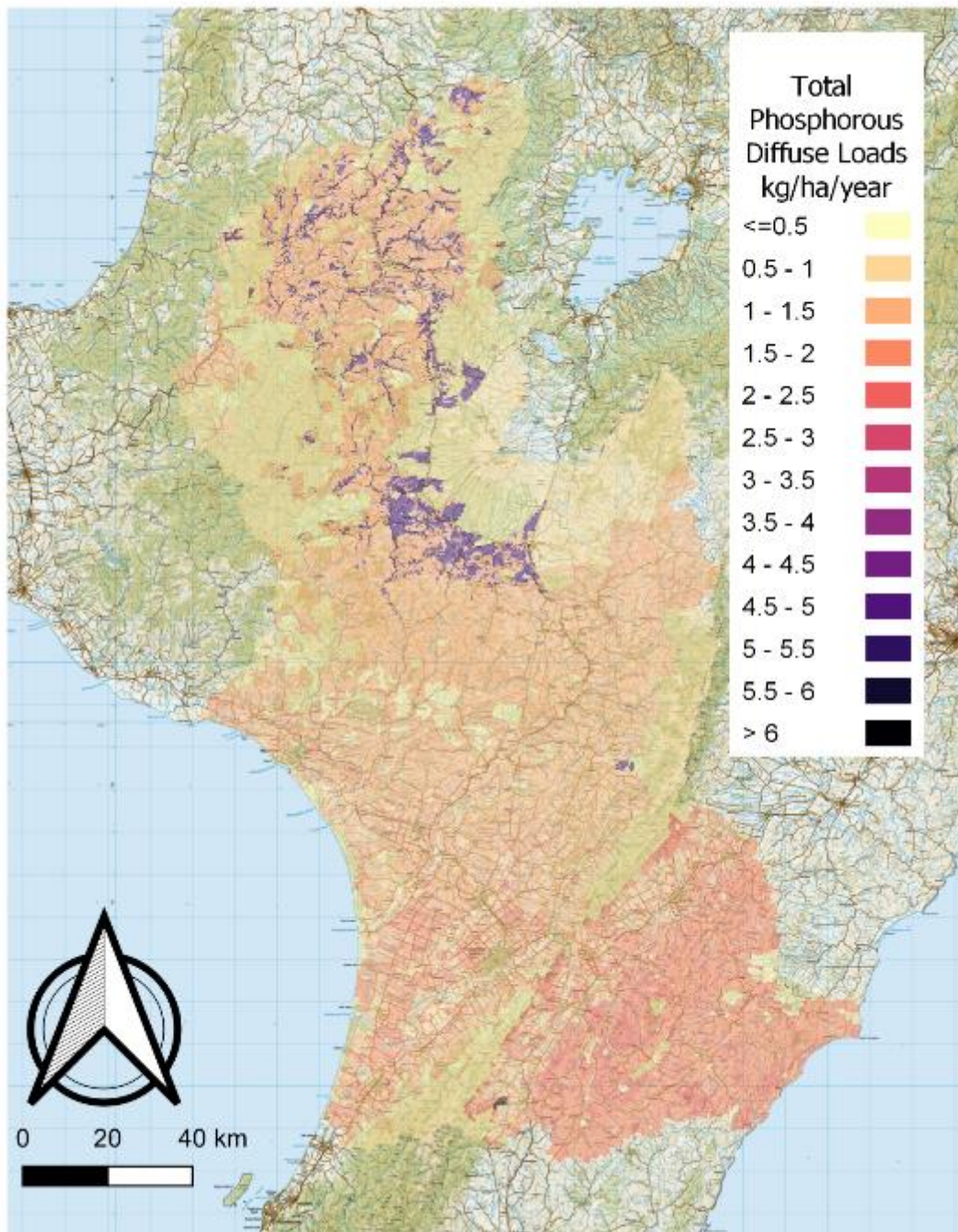


Figure 9. Total phosphorous diffuse source nutrient export coefficients.

2.6 Analysis of sediment erosion P

It has been documented elsewhere that P export coefficients, particularly when derived from OVERSEER, may be missing a significant portion of the total P export associated with infrequent, but largescale, erosion events (Parfitt et al. 2007, 2013; Gray et al. 2016). We refer to this portion of the total P export as sediment erosion P (SEP) and acknowledge that it is not represented by the model export coefficients described in Section 2.5. An analysis was therefore undertaken to better understand the importance of SEP in our catchment modelling and to support the model calibration described in Section 2.7.

Relevant background to this analysis is the recognition that the observed TP loads at the water quality monitoring sites are uncertain and, in fact, are likely under-estimates of the total TP instream loads. Under-estimation is likely because monitoring is based on punctual monthly sampling that poorly characterises TP concentrations under infrequent high-flow conditions (Snelder *et al.*, 2017). In other words, the observed loads include some, but not all, of the SEP. We refer to this portion of the total P export as “observable” sediment erosion P (OSEP) and we hypothesise that this can be quantified for water quality monitoring sites. Based on this conceptual model, it follows that $OSEP < SEP$. See Appendix B for details of an analysis that supports these assumptions.

Our definition of OSEP is based on a hypothesis that there exists a portion of the total sediment erosion P load that is observable at downstream monitoring sites but is missing from our model diffuse export P (DEP) calculations. This makes the quantity important for catchment modelling. If the quantity is included on one side of our model equations (the calibration targets defined by the observed TP loads) then it needs to be included on the other side of the equations (total modelled P export). We further hypothesise that there are physiographic explanations for the variation in OSEP across catchments. We expect OSEP to be greater in catchments with high erodibility and lower in catchments with low erodibility for two reasons: 1. total SEP, by definition, will vary this way; and 2. the *observable* portion of SEP may be greater in higher erodibility catchments, as erosion likely occurs over a greater portion of the flow regime. To investigate these hypotheses, we undertook an analysis based on comparing DEP (plus point source P loads, PSP) to observed TP loads.

The analysis of DEP, PSP, and observed TP loads was undertaken in three steps. First, we used each of the SCAMP basin models to calculate DEP+PSP at each monitoring site in the region. For this procedure, the SCAMP model attenuation coefficients were all set to zero so that DEP was unattenuated. Second, for each location, we subtracted [DEP + PSP] from the observed instream TP load. We refer to this value as the “residual TP”:

$$\text{residual TP} = \text{observed TP load} - [\text{DEP} + \text{PSP}] \quad \text{Equation 1}$$

Based on Equation 1, where [DEP + PSP] was greater than the observed load, the residual TP was negative. This was interpreted as a location where attenuation of DEP exceeded any OSEP. Where [DEP + PSP] was less than the observed load, the residual TP was positive. Positive residual TP was interpreted as locations where OSEP was > 0 and, in fact, exceeded DEP attenuation. As a third step, we evaluated correlations between the residual TP values and physiographic characteristics of the upstream catchment that would support the hypothesis that OSEP variability is correlated with erodibility. A range of catchment physiographic characteristics were included as explanatory (independent) variables that may be related to residual TP. These characteristics included mean catchment slope, stream order, relative land use class distributions (% dairy, % dry stock, % forested), and the TP yields estimated using SedNetNZ (Vale 2022) (hereafter SedNetNZ TP yield).

Results of this analysis are presented in Section 3.1. We interpreted support for our hypotheses as evidence that our conceptual model is valid and that OSEP needed to be represented by the models. When present, the OSEP load represents a missing P contribution in the setup of the SCAMP model (i.e., it is not accounted for by DEP and PSP). Therefore, when indicated by the above analysis, we represented the OSEP load with an additional term in the SCAMP TP models. The quantification of this OSEP load term is described below.

2.7 Model Calibration

The relevant parameters for each model were calibrated so that modelled downstream TN and TP loads adequately matched observed loads at all calibration points (i.e., river water quality monitoring sites). Calibration performance was assessed based on the percent difference between modelled and observed loads at the calibration points, with a targeted difference of $\leq 10\%$. A guiding principle of the calibration process was to trust observed data, to the extent possible, throughout the process, and to prioritise reproducing observed conditions (i.e., agreement between measured and modelled data). The primary calibration parameters were diffuse pathway attenuation coefficients for each model sub-catchment. Calibration proceeded from upstream to downstream with manual adjustments to upstream attenuation coefficients, for each calibration point, to achieve the calibration targets.

For TN, a small number of sites also required modest increases to the original export coefficients (i.e., the coefficients shown in Table 3, 4 and 5), within a plausible range, to achieve calibration targets. These export coefficient adjustments never extended outside the original range of values for each land use class as described in Section 2.5.

For a small number of calibration points, the TN calibration target ($\leq 10\%$) could not be achieved with the adjustments described above without invalidating the calibration at other sites. These cases are most likely attributable to uncertainty associated with the calculated quality monitoring site loads and/or uncertainty associated with the point source load estimates.

For TP, the calibration target could not be achieved at some calibration points with adjustments to attenuation and export coefficients (within plausible ranges) alone. At these calibration points, the analysis described above indicated that the observed loads include an OSEP load component and that inclusion of OSEP sub-catchment load terms was justified. We added these OSEP load terms in the form of sub-catchment yields ($\text{kg ha}^{-1} \text{ yr}^{-1}$) for each sub-catchment above the calibration points, as required to achieve an acceptable calibration. In other words, OSEP was treated as a second calibration parameter. For these sub-catchments, the sub-catchment DEP attenuation coefficients were set to the model default minimum (0.1). The OSEP yield terms, and DEP attenuation coefficient, were applied uniformly to all sub-catchments above a calibration point (and below an upstream previously calibrated site).

For sub-catchments without a downstream calibration point, OSEP yields, and DEP attenuation coefficients, were set using the regression model described in Sections 2.6 and 3.1, as a function of sub-catchment erodibility parameters (slope and SedNetNZ TP yield). Manipulation of Equation 1 (Section 2.6) provided estimates of observable instream TP load for unmonitored locations:

$$\text{observable TP load} = \text{residual TP} + [\text{DEP} + \text{PSP}] \quad \text{Equation 2}$$

where the residual TP is calculated using the regression model presented in Section 3.1. The estimated observable instream loads, calculated using Equation 2, were then used as

calibration targets for the unmonitored sub-catchments. In other words, we used the fitted physiographic-based regression model to estimate residual TP for unmonitored catchments. We then used the estimated residual TP, along with modelled DEP and PSP, to estimate the instream TP load, at the bottom of the sub-catchment, that would be observable (if the site was monitored). The estimated observable instream TP loads served as surrogate calibration targets, in lieu of actual observed loads. For sub-catchments where the estimated instream load indicated an OSEP load component (i.e., positive residual), the DEP attenuation coefficient was set to 0.1 and the OSEP yield term was calibrated (iteratively) to achieve an acceptable agreement between estimated and modelled instream loads. For those sub-catchments with a negative calculated residual TP, OSEP was set to 0, and the DEP attenuation coefficient was set to a value > 0.1 . We constrained the maximum OSEP loads for un-monitored locations to the maximum of the range of calibrated OSEP loads at the calibration sites (i.e., water quality monitoring sites). In other words, even if the application of the regression equation suggested an exceptionally high OSEP load for a given sub-catchment, the model OSEP yield was capped at the maximum calibrated value for the calibration sites. This approach was taken in recognition of the error inherent in the regression equation and a desire to maintain plausibility bounds as suggested by measured data. This aligns with the guiding principle of trusting, and prioritising, the water quality monitoring site measured data in the calibration process.

Note that OSEP loads are not subject to attenuation in the model. Also note that, for TP, no adjustments were made to the original export coefficients (i.e., the coefficients shown in Table 3, 4 and 5).

To summarise, the calibration process followed the steps listed below.

1. TN and TP model attenuation coefficients were calibrated independently of each other, in two separate calibration exercises. Each of the four basin models were also calibrated independently of each other.
2. The calibration was performed for each calibration point in sequence, moving from upstream to downstream.
3. For each calibration point, we attempted to uniformly adjust all upstream uncalibrated sub-catchment attenuation coefficients to achieve an acceptable match with the observed loads. For all sub-catchments, the allowable minimum attenuation coefficient was 0.1.
4. Calibration performance was assessed based on the difference between modelled and measured mean annual load at the calibration points. A modelled value within 10% of the measured value was deemed acceptable.
5. For TN, if an acceptable calibration couldn't be achieved with adjustments to sub-catchment attenuation coefficients alone, adjustments, were made to sub-catchment land use-based diffuse source export coefficients. For all TN models in this study, this step only ever involved an *increase* in export coefficients from original values (see Section 2.5), with sub-catchment attenuation coefficients set to their model minimum value (0.1). Adjusted export coefficients never exceeded the originally established maximum values (Section 2.5) within a given land use class. Note that all TP export coefficients were maintained at their original values, summarised in Table 3, Table 4, and Table 5.

6. For TN, for sub-catchments without a downstream calibration point, attenuation coefficients were assigned based on the calibrated values of nearest neighbour sub-catchments.
7. For TP, where applicable, OSEP yield terms were added to sub-catchments above calibration points to achieve acceptable calibration. The magnitudes of the OSEP yield terms were set iteratively, while holding associated attenuation coefficients at the model allowable minimum value (0.1).
8. For TP, for sub-catchments without a downstream calibration point, attenuation coefficients and OSEP yields were set using the regression model described in Sections 2.6 and 3.1. OSEP yields for sub-catchments without downstream calibration points were capped at the maximum of the range of calibrated OSEP yields. Similarly, attenuation coefficients for sub-catchments without downstream calibration points were capped at the maximum of the range of calibrated attenuation coefficients.

3 Results and Discussion

3.1 Analysis of Sediment Erosion P

Mean catchment slope and SedNetNZ TP yield (Vale et al. 2022) were significantly correlated with residual TP (as defined in Section 2.6 and expressed as a yield kg TP ha⁻¹ yr⁻¹), with Pearson correlation coefficients (*r*) of 0.45 and 0.44, respectively (Figure 12). When combined in a multiple variable linear regression model, these two variables had variance inflation factors (VIF) less than 2. This indicates that each variable represents unique information and that the signs of the fitted coefficients can be reliably interpreted as representing the directions of the explanatory variable's relationships with residual TP (Zuur *et al.*, 2010). Both explanatory variables had positive fitted coefficients (Table 6), and the model explained 28% of the variability in residual TP over all calibration points.

Table 6. Fitted coefficients for multiple variable linear regression model explaining the between calibration points variation in residual TP.

Explanatory variable	Coefficient	Standard error	P value
Intercept	-1.48	0.46	0.0025
SedNetNZ TP yield	2.05	0.90	0.0295
Mean catchment slope	0.28	0.14	0.047

This regression model combines two characteristics that reflect catchment erodibility and can be expected to influence the magnitude of OSEP load at a site. The model, therefore, makes mechanistic sense. Sites with higher modelled sediment yields (as represented by SedNetNZ TP yield), can be expected to have larger OSEP and, therefore, larger residual TP. This is consistent with the positive coefficient for the explanatory variable SedNetNZ TP yield (Table 6). Because steeper catchments have a greater transport capacity, sites with higher mean catchment slope can be expected to deliver a greater portion of their total sediment P load at lower flows. This means that sites with higher mean catchment slope can be expected to have a relatively large component of observed TP load attributable to SEP and, therefore, larger residual TP. This is consistent with the positive coefficient for the explanatory variable mean catchment slope (Table 6).

This analysis supports our hypothesis that the observed TP loads include a component that is attributable to SEP, which we have defined as the observable sediment erosion P (OSEP). The OSEP load represents a component of the P load that needs to be represented in the SCAMP model calibration.

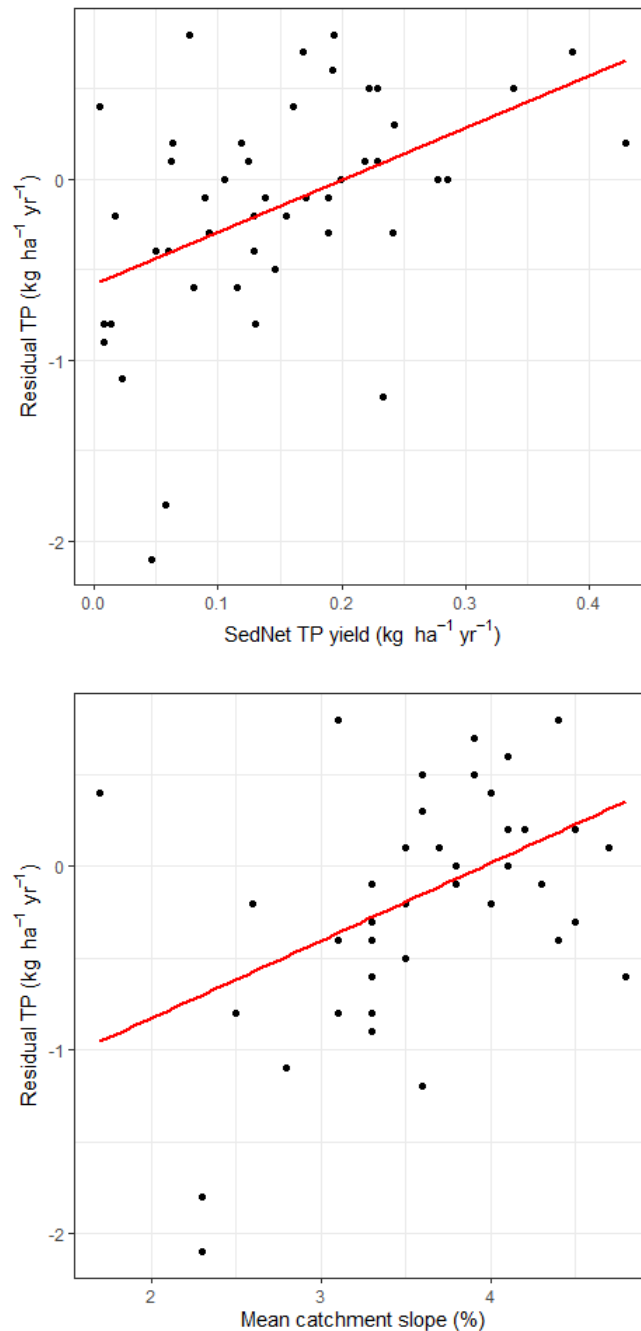


Figure 10. Correlation of residual TP with TP yields estimated using SedNetNZ (upper panel) and mean catchment slope (lower panel).

3.2 Model Calibration Results

Model calibration results are provided in Table 7 to Table 14. Summaries of calibrated diffuse pathway attenuation coefficients are shown in Figure 11 to Figure 20. Calibrated OSEP yield rates are summarised in Figure 21.

A satisfactory calibration was achieved for all four basin models and both nutrients (TN and TP). Most downstream calibration targets were achieved with allowable adjustments to upstream attenuation coefficients, within expected ranges, the addition of OSEP yields (TP

only), and, in a limited number of cases, minor adjustments to independently derived export coefficients (TN only). As noted above, for a small number of sites, calibration could not be achieved within the 10% target. These cases are likely attributable to the uncertainty of the observed (measured) loads. point sources (upstream and down) are responsible for the largest discrepancies between modelled and measured. For these sites, in such close proximity to each other, there are 3 sources of error: upstream site measurement error, point source discharge load estimate, and downstream site measurement error. The model is not capable of reconciling the errors at these particular sites. In other words, it was not possible to achieve both upstream and downstream site calibration targets given the assumed point source discharge load.

The calibration process attempted to maximise the number of sites where the calibration target was achieved, while maintaining plausible parameterisation, with priority placed on downstream sites.

A summary of the sources of the loads of TN and TP at the most downstream calibration point (i.e., water quality monitoring site) locations in each basin is provided in Figure 22. These pie charts show the proportional contribution (%), by major land use class and for point sources, to the total simulated instream load at the given river water quality site. Included here, for TP, are the total quantified contributions of observable sediment erosion P (i.e., OSEP), which are represented by the calibrated OSEP yield terms in the models.

Calibrated attenuation coefficients vary widely, both within a basin and across basins (Figure 11 to Figure 20). This is expected because variability in attenuation is driven by a range of factors including sub-catchment size, land cover, hydrology, and physiography, all of which are variable within and between the basins. A formal assessment of attenuation variability, patterns, or correlations between attenuation coefficients and catchment characteristics is beyond the scope of this study. Nitrogen attenuation is generally higher than phosphorus attenuation across all basins. Calibrated TN attenuation coefficients in the Manawatū, Rangitīkei, and Whangaehu River basins were $\geq 50\%$ for the majority of the drainage area. The Whanganui River basin exhibited the lowest TN attenuation of the four modelled basins, with calibrated attenuation coefficients $< 50\%$ for the majority of the drainage area.

Calibrated TP attenuation coefficients are typically $< 20\%$ for all four basins. The uncertainty associated with the calibrated TP attenuation coefficients is higher, as compared to TN attenuation, due to the OSEP terms. The need to account for OSEP in the calibration introduces a second “unknown” to the calibration process (OSEP yields) that reduces confidence in the two parameters values when considered independently. The two parameters can't be considered independently in the calibration process. This means that for each calibration site, there exists multiple combinations of upstream attenuation coefficients and OSEP yields that result in the same modelled instream load. However, past studies offer independent support of the derived values of the calibrated diffuse pathway attenuation coefficient for TP. A national application of the NIWA CLUES model quantified an average catchment-scale TP attenuation coefficient of 0.09 (Semadeni-Davies et al. 2020). This agrees well with our regional areal average of 0.18 and median of 0.10. For the Waikato River catchment, as part of the Plan Change 1 (PC1) process, an areal average TP catchment attenuation coefficient of 0.13 was quantified and used in modelling. For that same study, catchment “Sediment P” loads, analogous to our OSEP yields, were quantified and added to diffuse exports. The catchment areal average sediment P yield for PC1 was $0.3 \text{ kg ha}^{-1} \text{ yr}^{-1}$. This is comparable with our areal average modelled OSEP yield of $0.7 \text{ kg ha}^{-1} \text{ yr}^{-1}$.

Table 7. Comparison of calibrated Manawatū River basin model TN concentrations and loads with measured values.

Water Quality Site (Calibration Point)	Modelled (mg/L)	Measured (mg/L)	Modelled Load (t/y)	Measured (t/y)	% Difference
Manawatū at Weber Road	1.40	1.37	570.0	557.3	2%
Manawatū at Hopelands	1.19	1.19	1052.3	1050.8	0%
Manawatū at Ngawapurua Bridge	1.14	1.05	2306.7	2129.2	8%
Manawatū at Upper Gorge	1.05	1.09	2765.2	2870.2	-4%
Manawatū at Teachers College	0.98	0.96	3181.3	3109.2	2%
Manawatū at u/s PNCC STP	0.99	1.22	3251.1	3997.4	-19%
Manawatū at d/s PNCC STP	1.12	1.14	3732.7	3789.2	-1%
Manawatū at us Fonterra Longburn	1.14	1.11	3897.2	3794.5	3%
Manawatū at ds Fonterra Longburn	1.14	1.06	3897.3	3623.6	8%
Manawatū at Opiki Br	1.16	1.09	3930.0	3681.5	7%
Mangatoro at Mangahei Road	1.08	1.11	133.0	136.5	-3%
Kūmeti at Te Rehunga	1.66	1.79	21.0	22.6	-7%
Ōruakeretaki at S.H.2 Napier	1.98	2.11	93.5	99.8	-6%
Ōruakeretaki at d/s PPCS Oringi STP	1.98	1.87	93.8	88.5	6%
Raparapawai at Jackson Rd	1.42	1.38	40.4	39.2	3%
Mākuri i at Tuscan Hills	1.97	1.95	180.6	178.3	1%
Tiraumea at Ngāturi	1.55	1.69	677.3	740.8	-9%
Mangatainoka at Larsons Road	0.35	0.37	34.5	36.2	-5%
Mangatainoka at Brewery - S.H.2 Bridge	1.23	1.34	529.7	574.7	-8%
Mangatainoka at d/s DB Breweries	1.24	1.34	529.8	574.7	-8%
Mangahao at Ballance	0.44	0.47	197.4	209.0	-6%
Mangapapa at Troup Rd	1.49	1.40	23.5	22.1	6%
Mangaatua at u/s Woodville STP	0.89	1.21	47.9	64.9	-26%
Mangaatua at d/s Woodville STP	1.55	1.44	82.9	77.2	7%
Pohangina at Mais Reach	0.38	0.38	176.8	177.4	0%
Kahuterawa at Johnstons Rātā	0.81	0.86	20.4	21.7	-6%
Ōroua at Almadale Slackline	0.66	0.74	144.7	161.0	-10%
Ōroua at U/S AFFCO Feilding	0.90	0.80	322.1	285.1	13%
Ōroua at d/s AFFCO Feilding	0.90	0.92	322.1	327.8	-2%
Ōroua at U/S Feilding STP	0.96	1.31	342.7	466.8	-27%
Ōroua at d/s Feilding STP	1.84	2.05	657.0	730.5	-10%
Ōroua at Awahuri Bridge	1.71	1.37	679.9	544.4	25%
Tokomaru River at Horseshoe bend	0.39	0.39	23.6	23.4	1%
Manakau at S.H.1 Bridge	1.32	1.29	12.5	12.2	2%
Waikawa at North Manakau Road	0.20	0.22	8.8	9.7	-9%
Owahanga at Branscombe Bridge	1.22	1.26	222.8	230.5	-3%
Ōhau at Gladstone Reserve	0.24	0.26	43.4	47.6	-9%

Table 8. Comparison of calibrated Manawatū River basin model TP concentrations and loads with measured values.

Water Quality Site (Calibration Point)	Modelled (mg/L)	Measured (mg/L)	Modelled Load (t/y)	Measured (t/y)	% Difference
Manawatū at Weber Road	0.23	0.22	95.2	89.5	6.0%
Manawatū at Hopelands	0.19	0.14	167.4	123.6	36.3%
Manawatū at Ngawapurua Bridge	0.18	0.19	367.0	385.3	-9.2%
Manawatū at Upper Gorge	0.16	0.14	428.8	368.7	10.5%
Manawatū at Teachers College	0.21	0.24	688.9	777.3	-16.8%
Manawatū at u/s PNCC STP	0.21	0.23	691.4	753.6	-9.6%
Manawatū at d/s PNCC STP	0.22	0.19	732.4	631.5	14.4%
Manawatū at us Fonterra Longburn	0.22	0.2	749.2	683.7	8.1%
Manawatū at ds Fonterra Longburn	0.22	0.21	749.2	717.9	3.0%
Manawatū at Opiki Br	0.22	0.17	751.3	574.2	29.1%
Mangatoro at Mangahei Road	0.37	0.37	45.8	45.5	0.0%
Kūmeti at Te Rehunga	0.07	0.07	0.9	0.9	2.4%
Ōruakeretaki at S.H.2 Napier	0.10	0.1	4.7	4.7	1.2%
Ōruakeretaki at d/s PPCS Oringi STP	0.10	0.1	4.7	4.7	1.4%
Raparapawai at Jackson Rd	0.27	0.26	7.6	7.4	3.8%
Mākuri at Tuscan Hills	0.26	0.25	23.5	22.9	2.8%
Tiraumea at Ngāturi	0.25	0.26	111.6	114.0	-0.6%
Mangatainoka at Larsons Road	0.04	0.04	4.1	3.9	3.8%
Mangatainoka at Brewery - S.H.2 Bridge	0.09	0.08	36.7	34.3	7.1%
Mangatainoka at d/s DB Breweries	0.09	0.09	36.8	38.6	-4.7%
Mangahao at Balance	0.09	0.09	41.0	40.0	-8.1%
Mangapapa at Troup Rd	0.10	0.09	1.6	1.4	9.4%
Mangaatua at u/s Woodville STP	0.08	0.11	4.6	5.9	-22.8%
Mangaatua at d/s Woodville STP	0.14	0.13	7.3	7.0	5.2%
Pohangina at Mais Reach	0.09	0.09	41.2	42.0	1.9%
Kahuterawa at Johnstons Rātā	0.06	0.06	1.5	1.5	0.6%
Ōroua at Almadale Slackline	0.17	0.17	37.0	37.0	-4.7%
Ōroua at U/S AFFCO Feilding	0.18	0.27	62.4	96.2	-36.1%
Ōroua at d/s AFFCO Feilding	0.18	0.18	62.4	64.1	-4.2%
Ōroua at U/S Feilding STP	0.18	0.17	62.8	60.6	2.1%
Ōroua at d/s Feilding STP	0.18	0.14	63.7	49.9	25.8%
Ōroua at Awahuri Bridge	0.17	0.16	67.9	63.6	5.4%
Tokomaru River at Horseshoe bend	0.04	0.04	2.3	2.4	-2.8%
Manakau at S.H.1 Bridge	0.08	0.08	0.8	0.8	1.1%
Waikawa at North Manakau Road	0.02	0.02	0.9	0.9	2.4%
Owahanga at Branscombe Bridge	0.29	0.29	53.2	53.0	-0.2%
Ōhau at Gladstone Reserve	0.03	0.03	5.5	5.5	-3.0%

Table 9. Comparison of calibrated Rangitikei River basin model TN concentrations and loads with measured values.

Water Quality Site (Calibration Point)	Modelled (mg/L)	Measured (mg/L)	Modelled Load (t/y)	Measured (t/y)	% Difference
Rangitikei at Pukeokahu	0.21	0.21	158.0	158.3	-0.2%
Rangitikei at Mangaweka	0.39	0.38	823.5	801.7	2.7%
Rangitikei at Onepuhi	0.40	0.39	985.6	970.4	1.6%
Rangitikei at u/s Bulls STP	0.54	0.59	1435.0	1553.6	-7.6%
Rangitikei at us Riverlands STP	0.56	0.62	1473.6	1632.6	-9.7%
Rangitikei at McKelvies	0.68	0.63	1878.1	1730.5	8.5%
Hautapu at Papakai Road Bridge	0.77	0.56	116.7	109.0	7.1%
Hautapu at d/s Taihape STP	1.02	0.72	163.3	168.9	-3.3%
Hautapu at US Rangitikei River Conf	1.09	1.01	200.2	184.7	8.3%
Tūtaenui Stream at u/s Marton STP	3.50	3.69	110.5	116.4	-5.0%
Tūtaenui Stream at d/s Marton STP	4.36	3.27	137.4	103.1	33.3%

Table 10. Comparison of calibrated Rangitikei River basin model TP concentrations and loads with measured values.

Water Quality Site (Calibration Point)	Modelled (mg/L)	Measured (mg/L)	Modelled Load (t/y)	Measured (t/y)	% Difference
Rangitikei at Pukeokahu	0.03	0.03	24.8	22.6	9.8%
Rangitikei at Mangaweka	0.11	0.11	234.4	232.1	3.2%
Rangitikei at Onepuhi	0.14	0.14	353.4	348.3	3.3%
Rangitikei at u/s Bulls STP	0.18	0.25	474.4	658.3	-29.3%
Rangitikei at us Riverlands STP	0.18	0.19	487.1	500.3	-4.4%
Rangitikei at McKelvies	0.19	0.18	531.3	494.4	5.8%
Hautapu at Papakai Road Bridge	0.11	0.10	16.1	15.1	6.1%
Hautapu at d/s Taihape STP	0.16	0.16	26.1	25.7	-6.5%
Hautapu at US Rangitikei River Conf	0.15	0.14	28.1	25.6	1.8%
Tūtaenui Stream at u/s Marton STP	0.34	0.13	10.9	4.1	181.3%
Tūtaenui Stream at d/s Marton STP	0.52	0.52	16.3	16.4	3.4%

Table 11. Comparison of calibrated Whanganui River basin model TN concentrations and loads with measured values.

Water Quality Site (Calibration Point)	Modelled (mg/L)	Measured (mg/L)	Modelled Load (t/y)	Measured (t/y)	% Difference
Whanganui at Cherry Grove	0.33	0.35	439.6	466.9	-5.9%
Whanganui at u/s Taumarunui STP	0.49	0.35	1,205.7	862.0	39.9%
Whanganui at d/s Taumarunui STP	0.49	0.39	1,221.0	966.7	26.3%
Whanganui at Te Maire	0.56	0.61	1410.1	1,527.4	-7.7%
Whanganui at Wades Landing	0.79	0.86	3241.4	3536.6	-8.3%
Whanganui at Pipiriki	0.67	0.69	4366.1	4506.5	-3.1%
Whanganui at Te Rewa	0.71	0.68	5117.0	4870.0	5.1%
Whanganui at Paetawa	0.72	0.78	5117.0	5571.5	-8.2%
Whakapapa at Footbridge	0.05	0.05	17.7	18.1	-2.2%
Ōngarue at Taringamotu	0.67	0.73	758.3	828.8	-8.5%
Ōhura at Tokorima	0.97	0.98	732.0	741.7	-1.3%

Table 12. Comparison of calibrated Whanganui River basin model TP concentrations and loads with measured values.

Water Quality Site (Calibration Point)	Modelled (mg/L)	Measured (mg/L)	Modelled Load (t/y)	Measured (t/y)	% Difference
Whanganui at Cherry Grove	0.05	0.05	71.0	66.7	6.4%
Whanganui at u/s Taumarunui STP	0.06	0.02	145.9	49.3	196.3%
Whanganui at d/s Taumarunui STP	0.06	0.02	149.0	49.6	200.5%
Whanganui at Te Maire	0.08	0.08	198.9	200.3	0.2%
Whanganui at Wades Landing	0.10	0.10	416.5	411.2	0.5%
Whanganui at Pipiriki	0.14	0.14	919.9	914.4	-0.3%
Whanganui at Te Rewa	0.13	0.19	959.1	1360.7	0.6%
Whanganui at Paetawa	0.13	0.24	959.1	1714.3	-20.2%
Whakapapa at Footbridge	0.02	0.02	7.9	7.3	8.8%
Ōngarue at Taringamotu	0.07	0.06	74.2	68.1	8.9%
Ōhura at Tokorima	0.10	0.11	75.2	83.3	-9.7%

Table 13. Comparison of calibrated Whangaehu River basin model TN concentrations and loads with measured values.

Water Quality Station (Calibration Point)	Modelled (mg/L)	Measured (mg/L)	Modelled Load (t/y)	Measured (t/y)	% Difference
Whangaehu at Kauangaroa	0.78	0.78	1,108.2	1111.8	-0.3%
Mangaehuehu at d/s Rangataua STP	0.29	0.30	7.4	7.6	-2.4%
Mangaehuehu at u/s Rangataua STP	0.30	0.29	7.6	7.3	3.6%
Tokiahuru at Junction	0.21	0.20	53.7	50.5	6.3%
Makotuku at SH49A	0.22	0.22	7.0	6.9	0.4%
Makotuku at Raetihi	0.51	0.50	35.4	34.7	2.0%
Makotuku at Above Sewage Plant	0.47	0.49	35.4	37.1	-4.6%
Makotuku at d/s Raetihi STP	0.51	0.51	38.7	38.6	0.3%
Mangawhero at u/s Ohakune STP	0.50	0.49	45.8	44.8	2.2%
Mangawhero at d/s Ohakune STP	0.81	0.54	74.3	49.4	50.4%
Mangawhero at Pakihi Rd Bridge	0.53	0.53	86.0	85.2	0.9%
Mangawhero at Raupiu Road	0.38	0.38	213.2	212.1	0.5%
Turakina at ONeills Bridge	2.03	2.10	536.9	556.3	-3.5%

Table 14. Comparison of calibrated Whangaehu River basin model TP concentrations and loads with measured values.

Water Quality Site (Calibration Point)	Modelled (mg/L)	Measured (mg/L)	Modelled Load (t/y)	Measured (t/y)	% Difference
Whangaehu at Kauangaroa	0.21	0.21	299.0	299.3	1.8%
Mangaehuehu at d/s Rangataua STP	0.02	0.02	0.5	0.5	-4.0%
Mangaehuehu at u/s Rangataua STP	0.02	0.02	0.5	0.5	3.1%
Tokiahuru at Junction	0.05	0.05	12.6	12.6	-0.1%
Makotuku at SH49A	0.01	0.01	0.2	0.3	-2.2%
Makotuku at Raetihi	0.02	0.02	1.4	1.4	7.9%
Makotuku at Above Sewage Plant	0.02	0.02	1.4	1.5	-1.1%
Makotuku at d/s Raetihi STP	0.03	0.02	2.0	1.5	33.6%
Mangawhero at u/s Ohakune STP	0.03	0.05	2.6	4.6	-44.0%
Mangawhero at d/s Ohakune STP	0.08	0.08	7.6	7.3	3.5%
Mangawhero at Pakihi Rd Bridge	0.06	0.03	9.0	4.8	87.2%
Mangawhero at Raupiu Road	0.05	0.05	28.8	27.9	3.6%
Turakina at ONeills Bridge	0.51	0.51	135.9	135.1	-1.3%

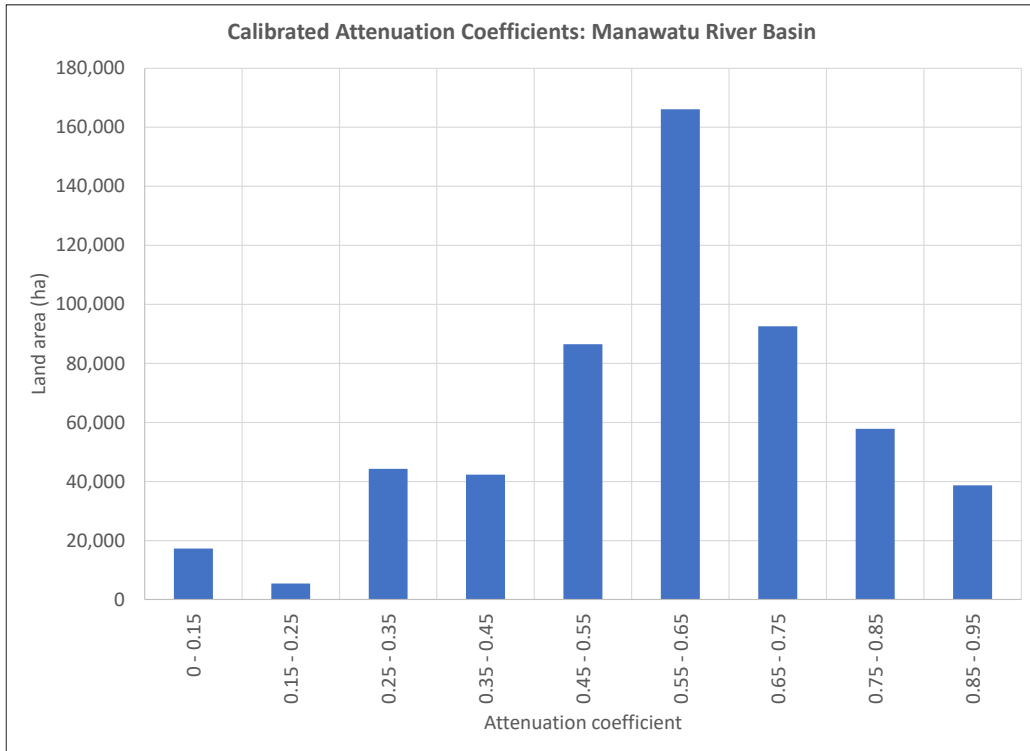


Figure 11. Areal distribution of calibrated diffuse pathway attenuation coefficients for TN, Manawātū River basin.

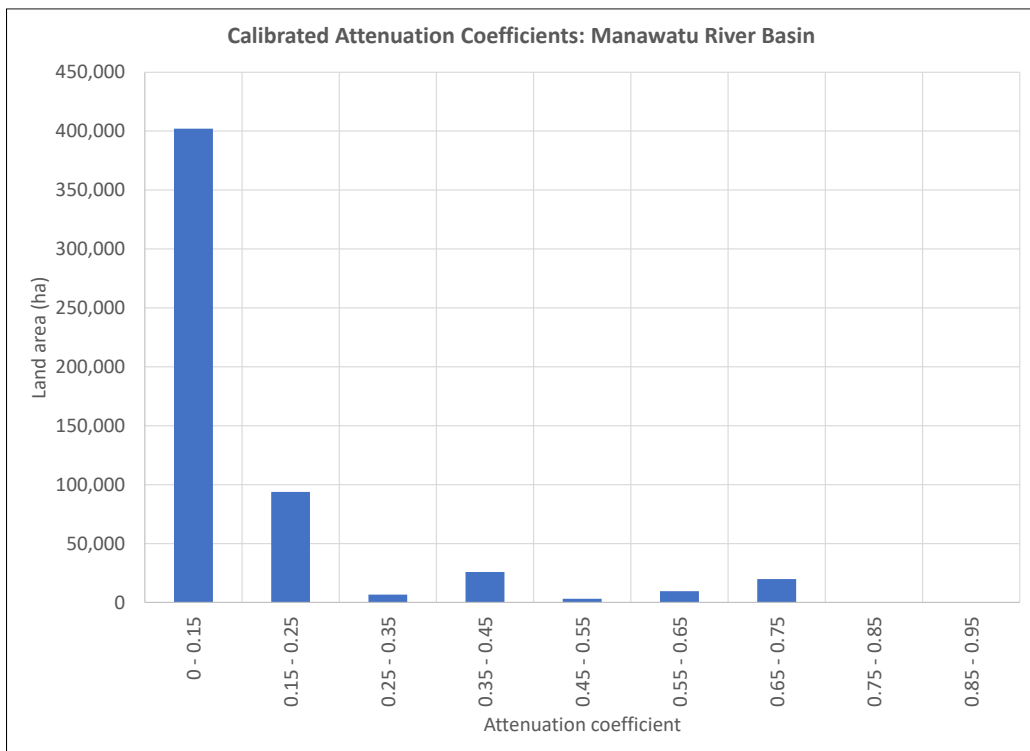


Figure 12. Areal distribution of calibrated diffuse pathway attenuation coefficients for TP, Manawātū River basin.

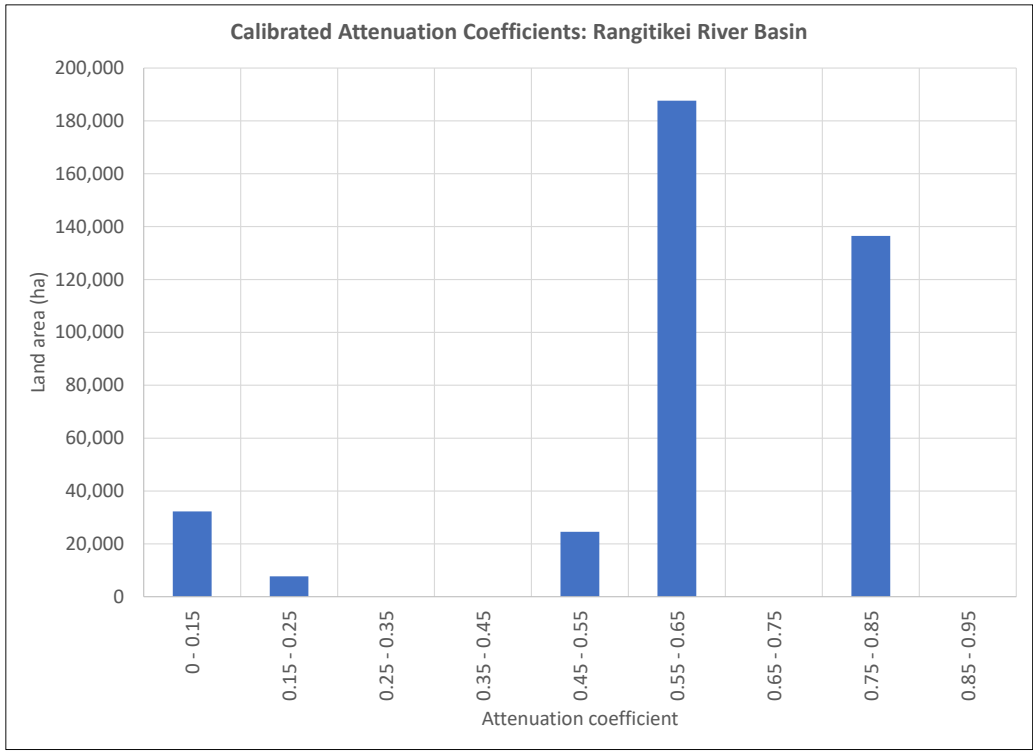


Figure 13. Areal distribution of calibrated diffuse pathway attenuation coefficients for TN, Rangitikei River basin.

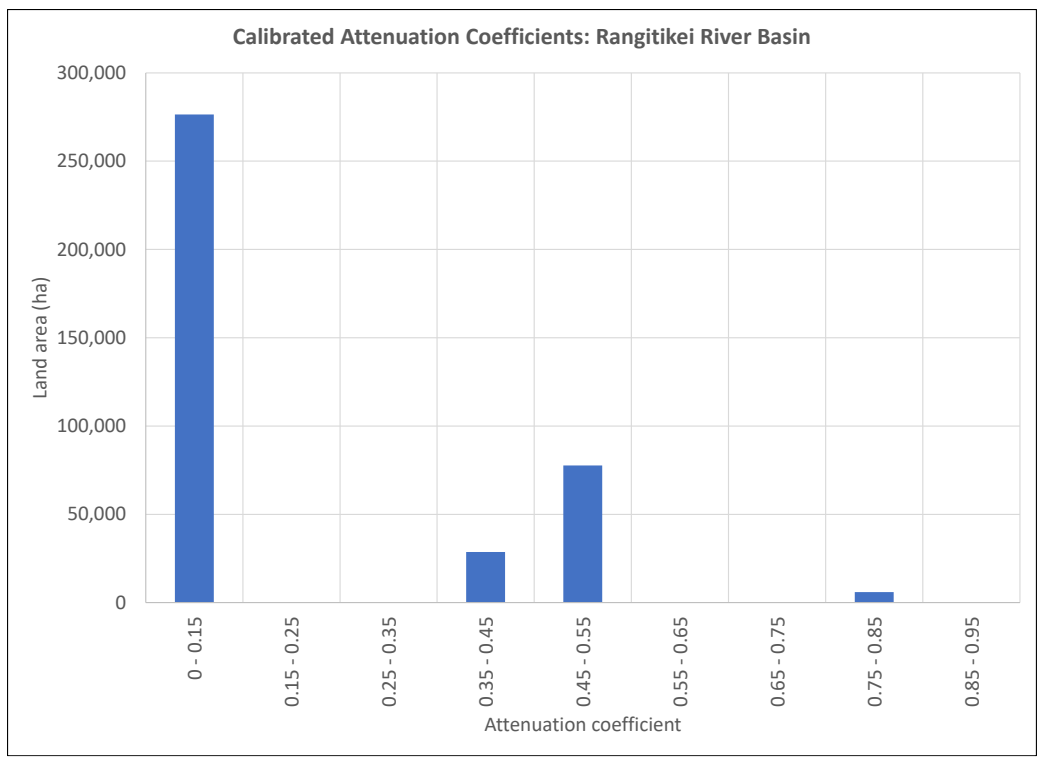


Figure 14. Areal distribution of calibrated diffuse pathway attenuation coefficients for TP, Rangitikei River basin.

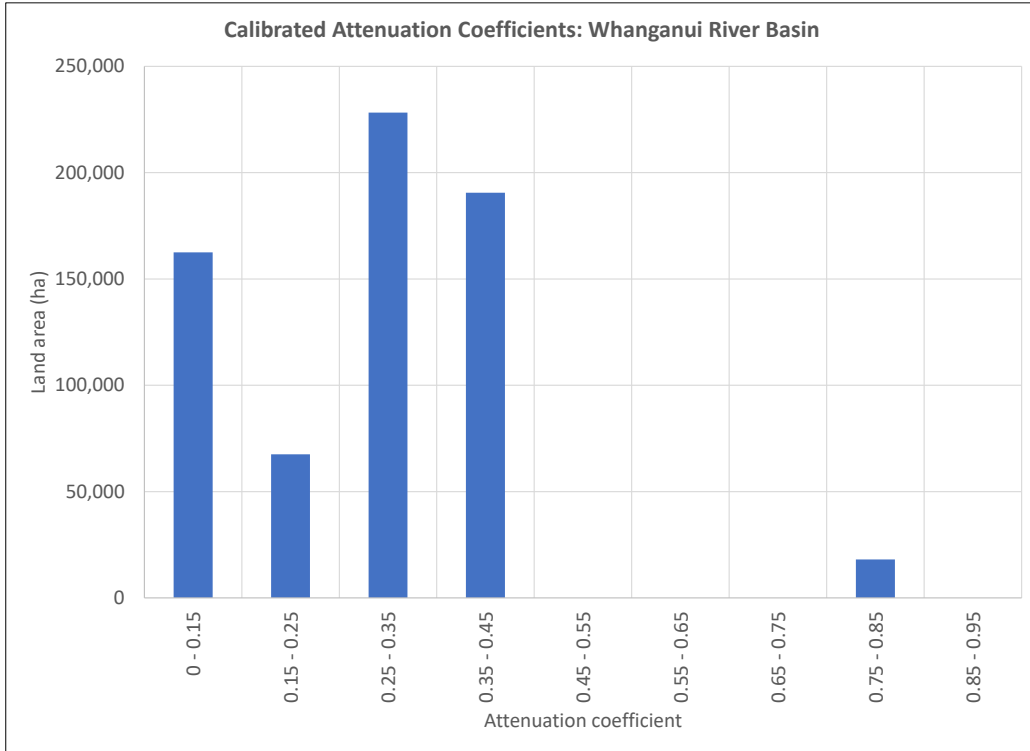


Figure 15. Areal distribution of calibrated diffuse pathway attenuation coefficients for TN, Whanganui River basin.

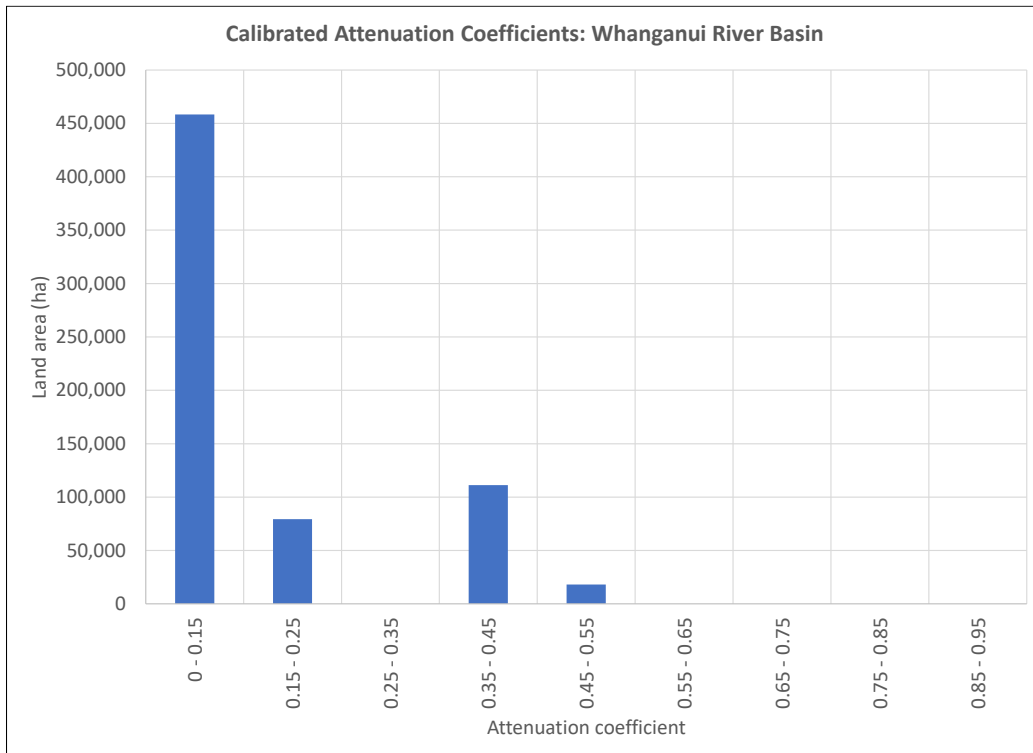


Figure 16. Areal distribution of calibrated diffuse pathway attenuation coefficients for TP, Whanganui River basin

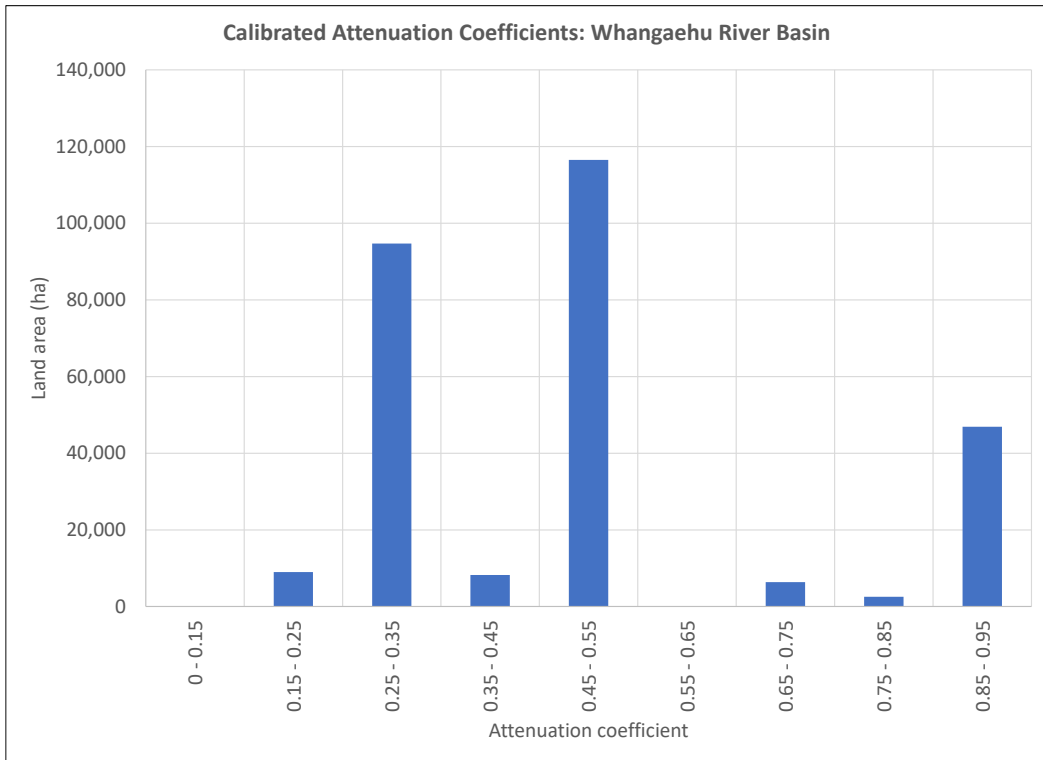


Figure 17. Areal distribution of calibrated diffuse pathway attenuation coefficients for TN, Whangaehu River basin.

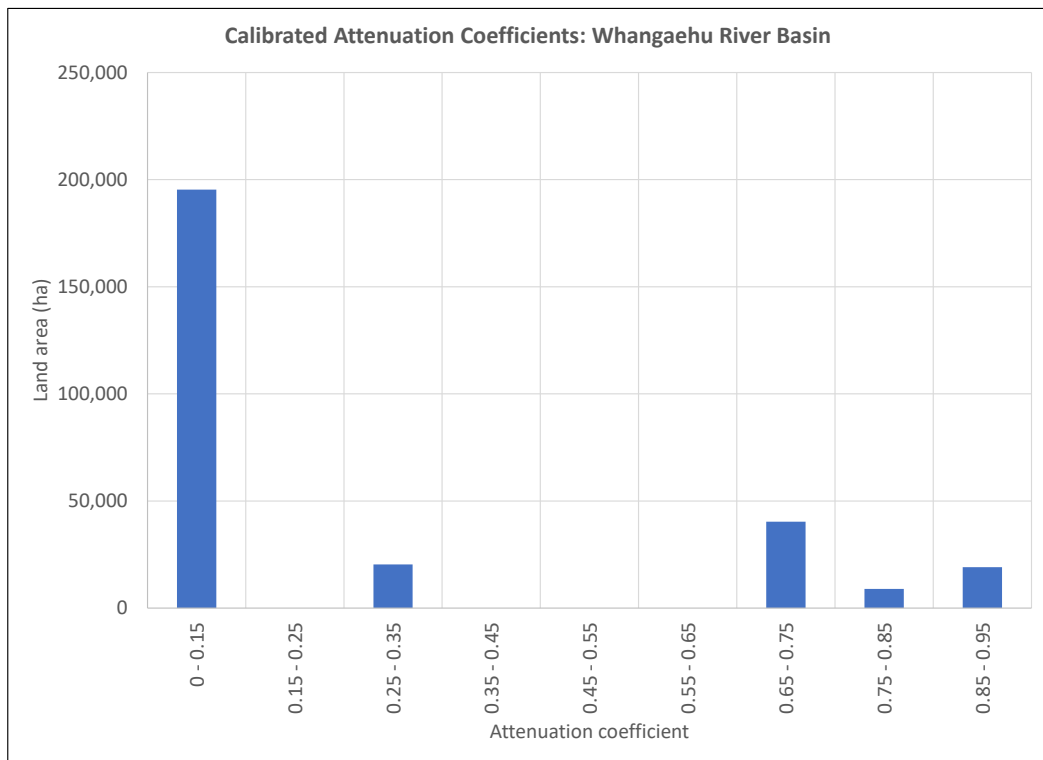


Figure 18. Areal distribution of calibrated diffuse pathway attenuation coefficients for TP, Whangaehu River basin.

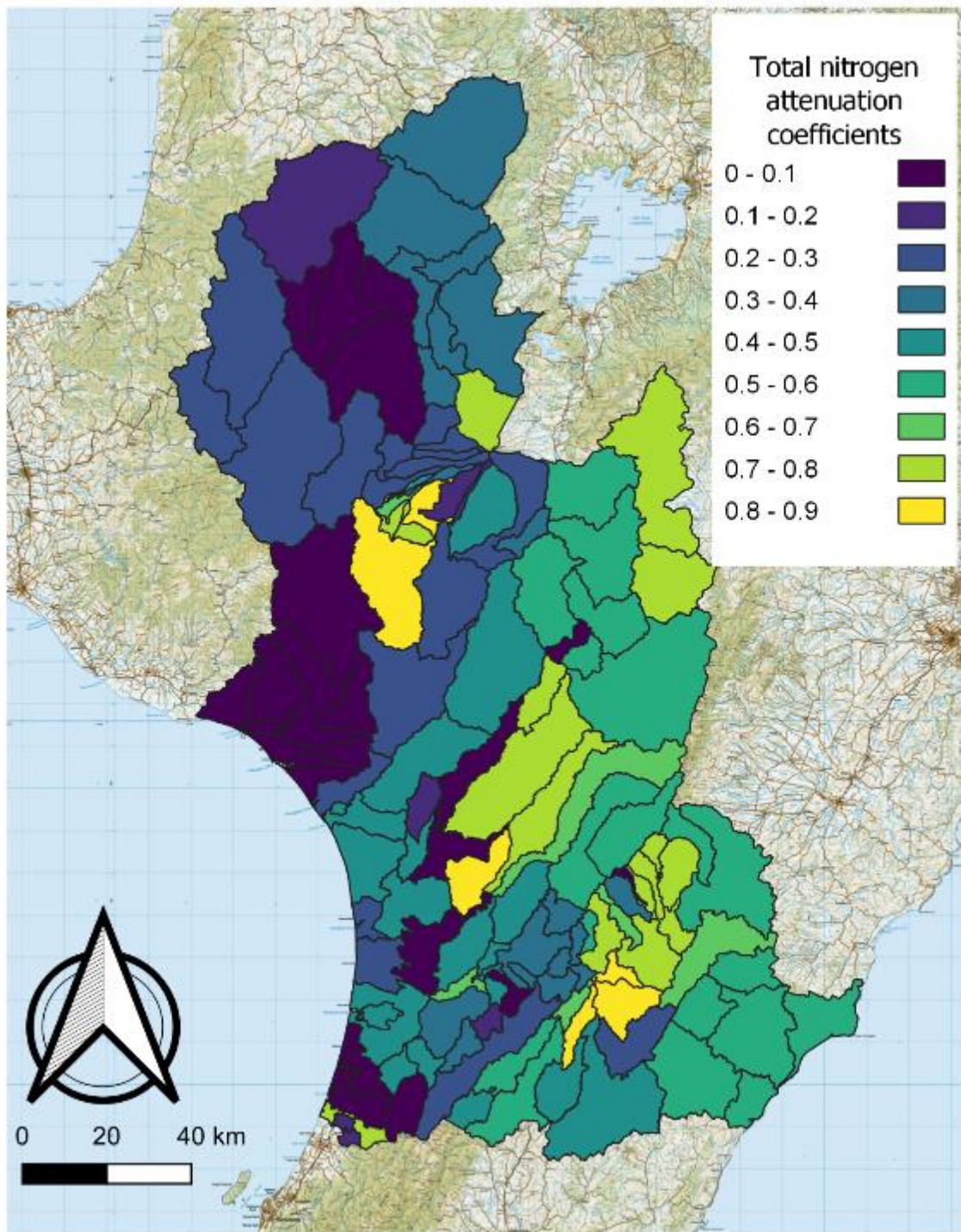


Figure 19. Total nitrogen calibrated diffuse pathway attenuation coefficients for each sub-catchment.

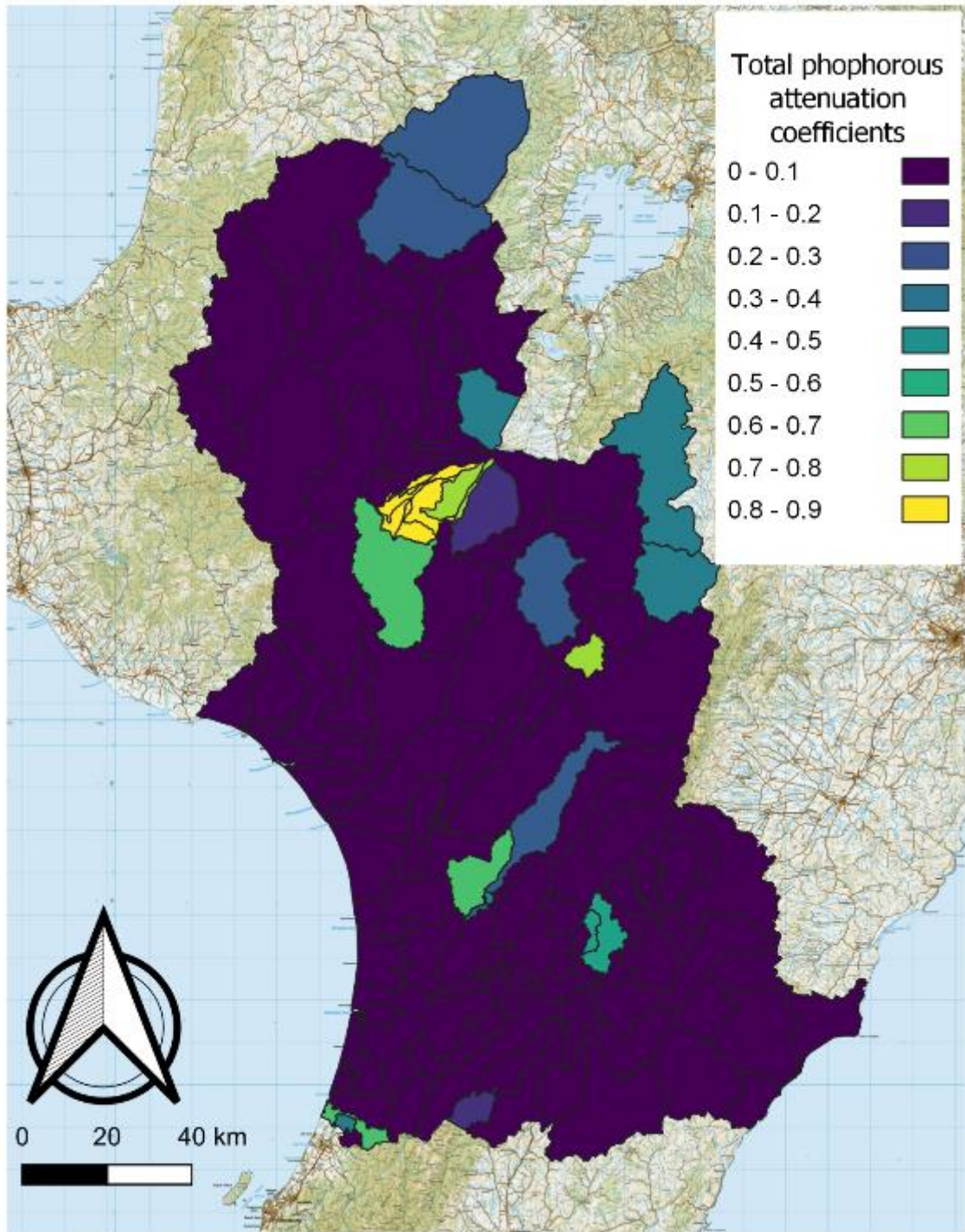


Figure 20. Total phosphorus calibrated diffuse pathway attenuation coefficients for each sub-catchment.

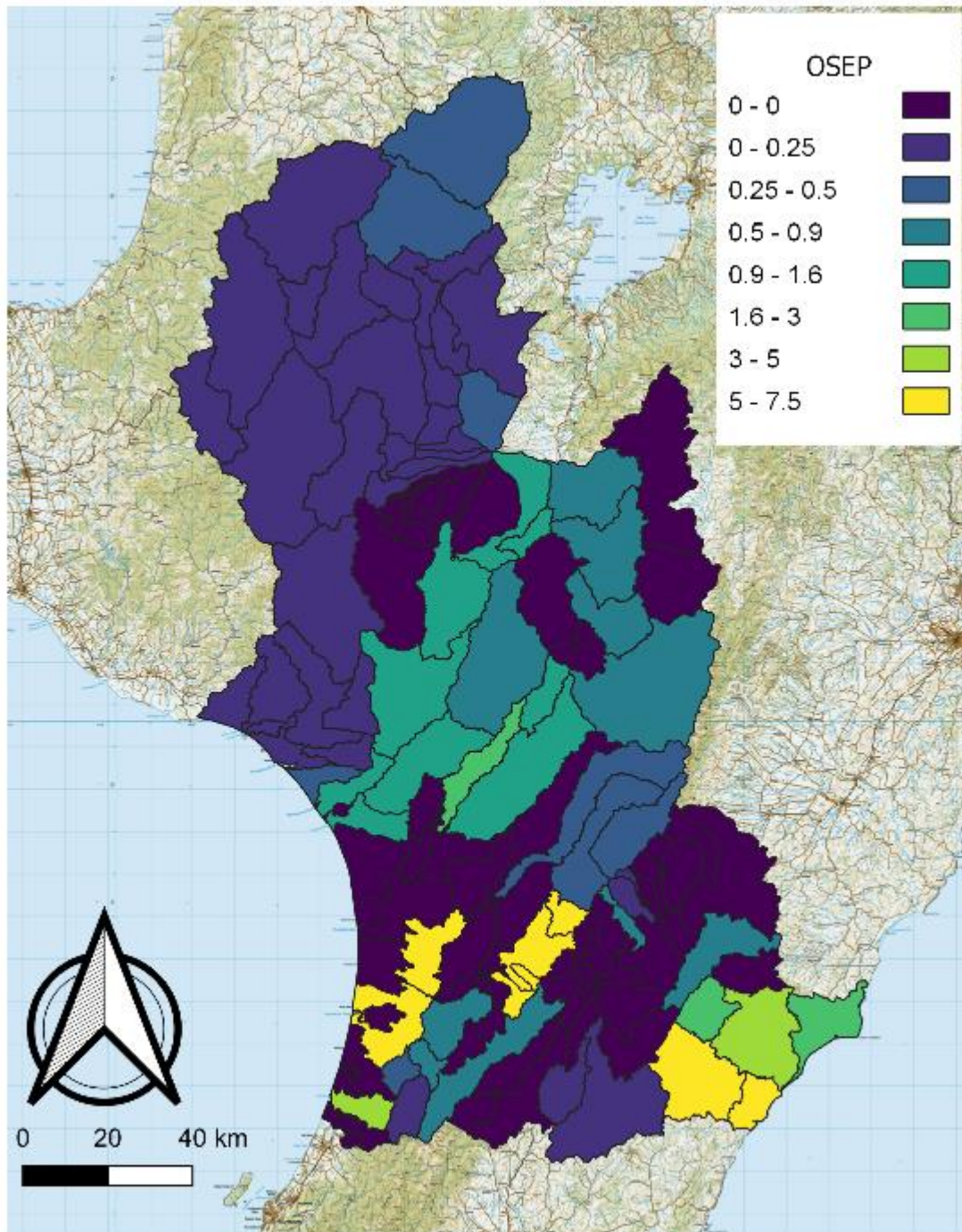


Figure 21. Calibrated observed sediment erosion phosphorus (OSEP) sub-catchment yields (kg ha⁻¹ year⁻¹).

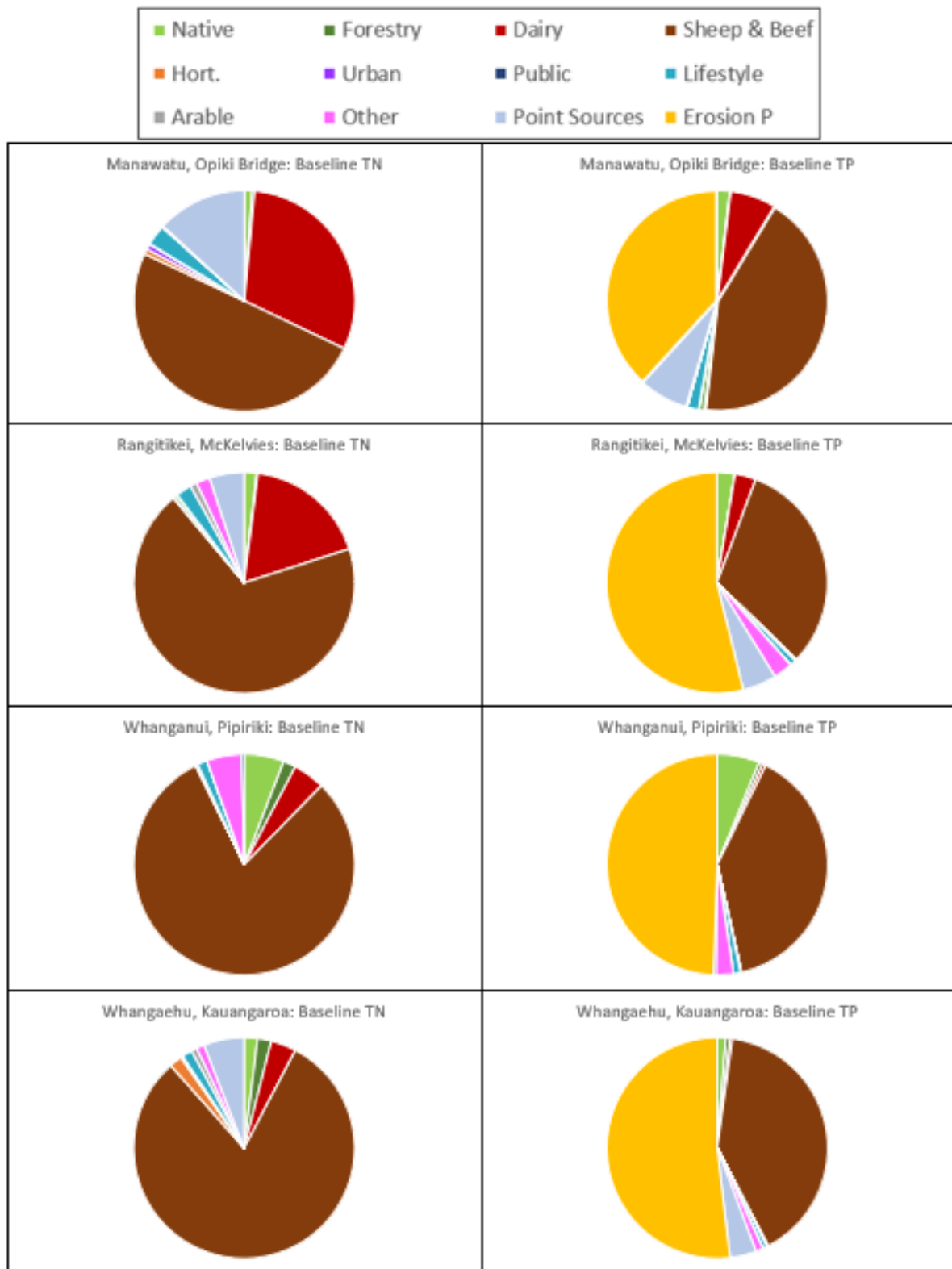


Figure 22. Summary of source load distributions for downstream sites in modelled river basins.

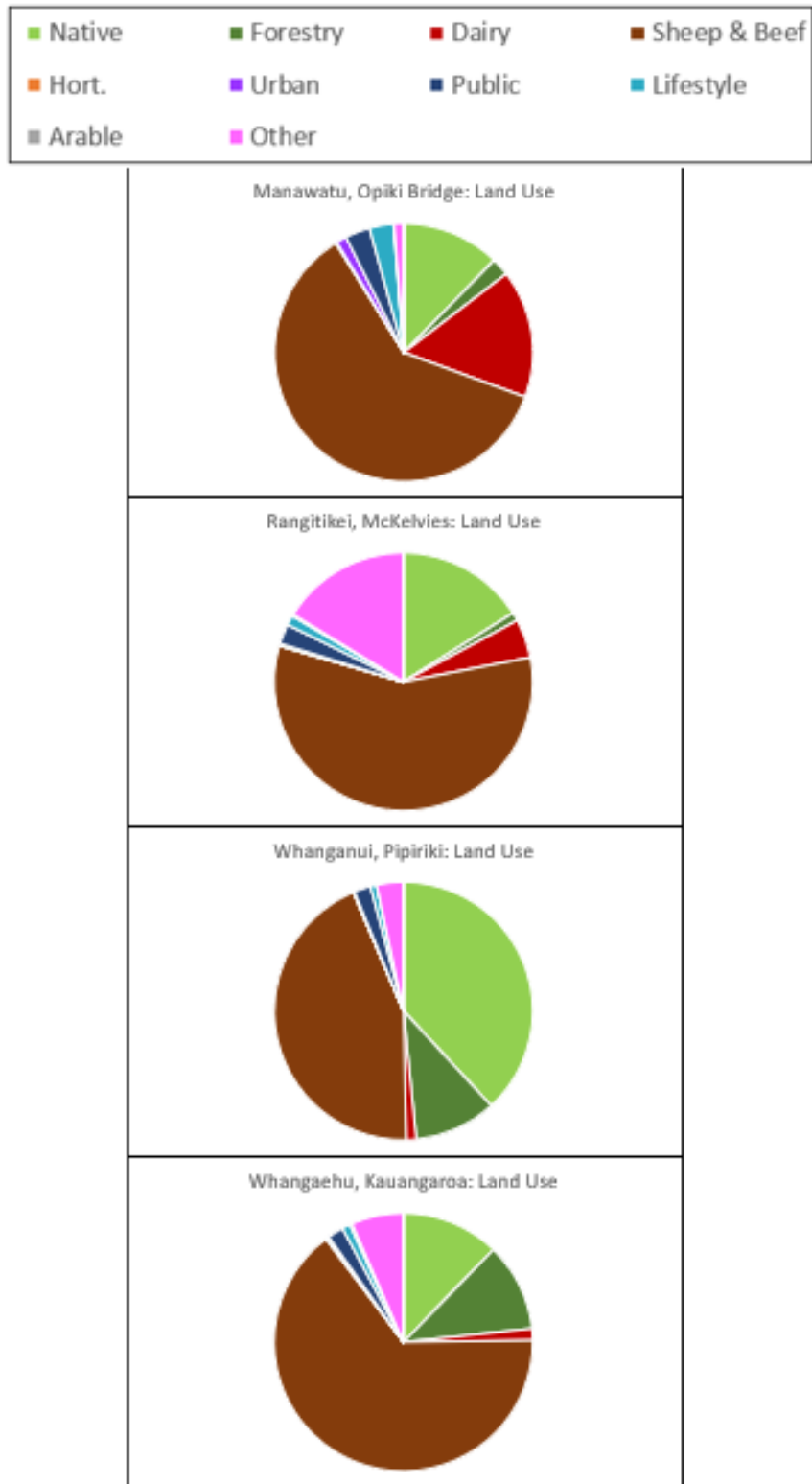


Figure 23. Summary of land use distributions for downstream sites in modelled river basins.

Table 15. Baseline model TN source load distributions for example model locations

Land use Class	Example model locations			
	Manawatū at Opiki Bridge	Rangitīkei at McKelvies	Whanganui at Pipiriki	Whangaehu at Kauangaroa
Native	1.1%	1.8%	5.8%	1.9%
Forestry	0.4%	0.2%	1.8%	2.0%
Dairy	30.6%	18.0%	4.7%	3.7%
Sheep & Beef	49.9%	68.9%	80.4%	80.8%
Horticulture	0.8%	0.2%	0.0%	1.9%
Urban	0.8%	0.4%	0.1%	0.2%
Public	0.1%	0.1%	0.2%	0.1%
Lifestyle	3.0%	2.3%	1.4%	1.5%
Arable	0.1%	1.0%	0.0%	0.8%
Other	0.1%	2.0%	5.1%	1.1%
Point Sources	13.2%	5.1%	0.4%	5.9%

Table 16. Baseline model TP source load distributions for example model locations.

Land use Class	Example model locations			
	Manawatū at Opiki Bridge	Rangitīkei at McKelvies	Whanganui at Pipiriki	Whangaehu at Kauangaroa
Native	1.8%	2.6%	6.2%	1.2%
Forestry	0.1%	0.1%	0.6%	0.6%
Dairy	6.7%	3.1%	0.5%	0.4%
Sheep & Beef	43.1%	31.5%	39.2%	40.2%
Horticulture	0.1%	0.0%	0.0%	0.2%
Urban	0.7%	0.2%	0.1%	0.0%
Public	0.1%	0.1%	0.1%	0.1%
Lifestyle	1.7%	0.9%	1.0%	0.6%
Arable	0.0%	0.0%	0.0%	0.0%
Other	0.1%	2.8%	2.5%	1.1%
Point Sources	7.2%	5.0%	0.3%	3.9%
Sediment Erosion	38.2%	53.8%	49.5%	51.8%

4 Summary and conclusion

Catchment water quality models representing loads and concentrations of TN and TP were developed for four major river basins in the Horizons Region: the Manawatū, the Rangitīkei, the Whanganui, and the Whangaehu. The models use sub-catchment export and attenuation coefficients to simulate the generation, transport, and downstream delivery of total nitrogen and total phosphorus loads throughout the Horizons region. The models were developed to support regional nutrient management and planning and can be used in future to simulate the impact of a wide range of land use and management scenarios on nitrogen and phosphorus loads and concentrations throughout the region. The models were developed in a usable framework to allow for future application by a range of potential end users.

Satisfactory calibration was achieved for all four basin models. Downstream calibration targets were achieved for most locations with adjustments to upstream attenuation coefficients, within expected ranges, the addition of OSEP yield terms (TP only), and, for TN and a small number of sites, adjustments to independently derived export coefficients. In general, calibrated nitrogen attenuation coefficients are higher than phosphorus attenuation coefficients. Phosphorus attenuation coefficient values are less certain than nitrogen attenuation coefficient values because of the introduction of an additional unknown (OSEP yield terms) to the calibration process.

We consider the 8 models (i.e., four basins representing TN and TP) to be well-calibrated and represent the best available science for predicting catchment water quality responses to changes in land use and/or practices, or point sources, given the available knowledge, information and data. The models make the best use of available data to the extent practicable. That said, there are uncertainties associated with the models that limit how the models should be used. Sources of uncertainty include the internal model parameterisation and the calibration process, the supporting data sets (e.g., land use data, water quality data, flow data), and the simplified model construct (e.g., lumped attenuation coefficients). A formal analysis of model uncertainty is possible with the SCAMP models but was beyond the scope of this study. However, the uncertainty needs to be borne in mind when using the models to run simulations to inform decision-making.

The uncertainty associated with model TP predictions is higher than that associated with TN predictions. This is because of the sediment erosion P (SEP), which is believed to be largely missing from model export coefficients and partially missing from observed instream loads. To account for this, observable sediment erosion P (OSEP) was added to the models as an additional calibration parameter. We are not able to estimate this parameter directly, because we don't know how much SEP is represented by the export coefficients nor how much is missing from the instream load estimates. In other words, the sub-catchment OSEP parameters represent an additional "unknown" in the model calculations and in the calibration process. This makes the final calibrated parameter set for TP less certain than the TN model. Future applications of the models, for predictive purposes, should be cognisant of this uncertainty and draw conclusions from the results accordingly. In any simulation, it is our opinion that DEP, PSP, and OSEP should be considered separately for accurate inclusion in mitigation simulations. For example, some potential mitigation actions may affect DEP but not OSEP or PSP; and vice versa. To address model TP uncertainty, future predictive simulations might employ formal uncertainty analyses, potentially utilising the software stochastic mode of simulation. This is left for future consideration.

The uncertainties associated with both TN and TP predictions at uncalibrated sites are higher than those associated with predictions at the calibration sites (i.e., the water quality monitoring

stations). This is because we had to rely on subjective “nearest neighbour” assignments and/or an imperfect supplemental regression model, rather than measured data, to estimate model attenuation (and OSEP) parameters at these locations. We recommend that future predictive applications of the model, to the extent possible, focus on results at calibration points rather than at uncalibrated assessment sites.

In addition to the nearest neighbour assignments, subjectivity, in the form of best professional judgement, was required at other steps in the calibration process. At all times, we maintained nutrient attenuation coefficients within the software’s default range (0.1 – 0.9). This decision was relevant to the TP calibration, where values had to be assigned for two unknowns (attenuation coefficient and OSEP) based on a single mass balance equation. This presented a condition of “equifinality”, where multiple combinations of upstream attenuation coefficients and OSEP yields result in the same modelled instream load. This was unavoidable due to the lack of available measured data associated with discrete P sources and pathways and the limitations of available supporting models (e.g., OVERSEER). Such conditions are common to numerical modelling exercises, especially with more complex models. Indeed, a more complex catchment model would only exacerbate the equifinality challenge in this study and would not add predictive power or reduce uncertainty. There are gaps in available data, and process understanding, required to support a more complex modelling approach. In our approach, where calculated “residual TP” (Equation 1) was negative, we set OSEP to 0 and adjusted the relevant attenuation coefficients (≥ 0.1) to achieve an acceptable calibration. Where the residual was positive, we set the upstream attenuation coefficients to 0.1 and adjusted the OSEP yields to achieve an acceptable calibration. These were subjective decisions; we could have achieved the same calibration performance results by assigning a combination of higher attenuation coefficients and larger OSEP yields. The decision to maintain a low TP attenuation coefficient was based on previous modelling experience, and published studies. The final element of subjectivity in the model parameterisation process was capping OSEP yields for sub-catchments without downstream calibration sites (i.e., uncalibrated sub-catchments). We capped these yields at the maximum value quantified for calibrated sub-catchments. We took this approach, in line with the guiding principle to trust, and prioritise, measured data over the predictions made using the supporting regression model.

It is also important to recognise that there is a portion of the total catchment P load that is not represented by the calibrated models at all. The evidence for this is analysis presented in Appendix B that indicates the observed instream TP loads under-estimate the total catchment P load (where the observed TP loads were the calibration targets). We consider that a proportion of the total catchment P load is not “observable” because it is associated primarily with high concentration, high flow events. Measurements during high flows have not been made by the routine state of environment monitoring that has supplied the data used to calculate the observed loads. As discussed above, we believe our instream observed load estimates under-represent the total P export because they under-estimate the sediment erosion P loads. However, this does not impact the utility of the model because the unobserved sediment erosion P loads, by definition, do not impact the regulatory river and stream concentrations of concern (observed mean and/or median concentrations).

Lastly, the absolute values of loads and concentrations predicted for a scenario should be regarded as less certain than the relative changes between scenarios. Like most models, these catchment models are better suited for predicting relative changes in basin water quality rather than absolute values. In other words, it may be wise to frame future scenario simulation results in terms of relative changes compared to the “baseline” (i.e., calibrated) models. Any

underlying model bias is effectively negated when considering relative differences in values. These statements are particularly true for unmonitored output assessment points. Confidence is higher in model predictions for the calibration points (i.e., water quality monitoring sites). In addition, applying relative (e.g., percentage) changes to model input parameters (e.g., export coefficients) will generally be a more defensible approach for scenario simulations than prescribing absolute values.

5 Acknowledgements

We thank Maree Patterson of Horizons Regional Council for assistance with data and reviews of early versions of this report. We thank Hugh Smith (MWLR) and Richard McDowell (AgResearch) for discussion around sediment sourced phosphorus.

6 References

- AgResearch, 2016. Estimates of nitrogen, phosphorus and sediment losses from selected source areas in the Mangatainoka catchment. Report No. 2016/EXT/1440. Prepared for Horizons Regional Council.
- Cohn, T.A., 2005. Estimating Contaminant Loads in Rivers: An Application of Adjusted Maximum Likelihood to Type 1 Censored Data. *Water Resources Research* 41. <http://onlinelibrary.wiley.com/doi/10.1029/2004WR003833/full>. Accessed 21 Jan 2016.
- Cohn, T.A., D.L. Caulder, E.J. Gilroy, L.D. Zynjuk, and R.M. Summers, 1992. The Validity of a Simple Statistical Model for Estimating Fluvial Constituent Loads: An Empirical Study Involving Nutrient Loads Entering Chesapeake Bay. *Water Resources Research* 28:2353–2363.
- Cohn, T.A., L.L. Delong, E.J. Gilroy, R.M. Hirsch, and D.K. Wells, 1989. Estimating Constituent Loads. *Water Resources Research* 25:937–942.
- Duan, N., 1983. Smearing Estimate: A Nonparametric Retransformation Method. *Journal of the American Statistical Association* 78:605–610.
- Dymond, J.R., A. Herzig, L. Basher, H.D. Betts, M. Marden, C.J. Phillips, A.-G.E. Ausseil, D.J. Palmer, M. Clark, and J. Roygard, 2016. Development of a New Zealand SedNet Model for Assessment of Catchment-Wide Soil-Conservation Works. *Geomorphology* 257:85–93.
- Efron, B., 1981. Nonparametric Estimates of Standard Error: The Jackknife, the Bootstrap and Other Methods. *Biometrika* 68:589–599.
- Fraser, C.E. and T. Snelder, 2019. Test of Methods for Calculating Contaminant Loads in the Manawatū-Whanganui Region: Supplementary Report. LWP Ltd, Christchurch.
- Fraser, C.E. and T. Snelder, 2020. Relationships between Instream Concentrations and River Nutrient Loads. LWP Client Report, LWP Ltd, Christchurch, New Zealand.
- Herzig, A., A. Manderson, B. Jolly, B. Barnes, and L. Baish, 2020. Opportunities and Constraints on Intensive Land-Use Expansion in the Horizons Region – Land-Use Mapping. MWLR Contract Report, Manaaki Whenua – Landcare Research, Palmerston North, New Zealand.
- McDowell, R.W., R.M. Monaghan, C. Smith, A. Manderson, L. Basher, D.F. Burger, S. Laurenson, P. Pletnyakov, R. Spiekermann, and C. Depree, 2021. Quantifying Contaminant Losses to Water from Pastoral Land Uses in New Zealand III. What Could Be Achieved by 2035? *New Zealand Journal of Agricultural Research* 64:390–410.
- NZ Government, 2020. National Policy Statement for Freshwater Management 2020.
- Parfitt, R.L., M. Frelat, J.R. Dymond, M. Clark, and J. Roygard, 2013. Sources of Phosphorus in Two Subcatchments of the Manawatu River, and Discussion of Mitigation Measures to Reduce the Phosphorus Load. *New Zealand Journal of Agricultural Research* 56:187–202.

- Roygard, J.K.F., K.J. McArthur, and M.E. Clark, 2012. Diffuse Contributions Dominate over Point Sources of Soluble Nutrients in Two Sub-Catchments of the Manawatu River, New Zealand. *New Zealand Journal of Marine and Freshwater Research* 46:219–241.
- Snelder, T.H., R.W. McDowell, and C.E. Fraser, 2017. Estimation of Catchment Nutrient Loads in New Zealand Using Monthly Water Quality Monitoring Data. *JAWRA Journal of the American Water Resources Association* 53:158–178.
- Vale, S., H. Smith, A. Neverman, and A. Herzig, No date. Stage 1 Data Delivery for Project “Application of SedNetNZ with SLUI Implementation to Support NPS-FM 2020 for Horizons Region”. Landcare Research Client report, Landcare Research.
- Zuur, A.F., E.N. Ieno, and C.S. Elphick, 2010. A Protocol for Data Exploration to Avoid Common Statistical Problems. *Methods in Ecology and Evolution* 1:3–14.

Appendix A Water quality site load calculations

A1 General approach

Mean annual TN and TP loads at all water quality sites were derived from monthly TN and TP concentrations and observed or modelled daily flows. Load calculation methods generally comprise two steps: (1) the generation of a series of flow and concentration pairs representing 'unit loads' and (2) the summation of the unit loads over time to obtain the total load. In practice step 1 precedes step 2 but in the explanation that follows, we describe step 2 first.

If flow and concentration observations were available for each day, the export coefficient, (the mean annual load, standardised by the upstream catchment area) would be the summation of the daily flows multiplied by their corresponding concentrations:

$$L = \frac{K}{A_c N} \sum_{j=1}^N C_j Q_j \quad (\text{Equation 1})$$

where L : mean annual export coefficient ($\text{kg yr}^{-1} \text{ha}^{-1}$), A_c : catchment area, ha, K : units conversion factor ($31.6 \text{ kg s mg}^{-1} \text{ yr}^{-1}$), C_j : contaminant concentration for each day in period of record (mg m^{-3}), Q_j : daily mean flow for each day in period of record ($\text{m}^3 \text{ s}^{-1}$), and N : number of days in period of record.

In this summation, the individual products represent unit loads. Because concentration data are generally only available for infrequent days (i.e., generally in this study, monthly observations), unit loads can only be calculated for these days. However, flow is generally observed continuously, or the distribution of flows can be estimated for locations without continuous flow data, and there are often relationships between concentration and flow, time and/or season. Rating curves exploit these relationships by deriving a relationship between the sampled nutrient concentrations (c) and simultaneous observations of flow (q). Depending on the approach, relationships between concentration and time and season may be included in the rating curve. This rating curve is then used to generate a series of flow and concentration pairs (i.e., to represent Q_j and C_j in equation 1) for each day of the entire sampling period (i.e., step 1 of the calculation method; Cohn *et al.*, 1989). The estimated flow and concentration pairs are then multiplied to estimate unit loads, and these are then summed and transformed by K , N and A_c to estimate mean annual export coefficients (i.e., step 2 of the calculation method; Equation 1).

There are a variety of approaches to defining rating curves. Identifying the most appropriate approach to defining the rating curve requires careful inspection of the available data for each site and contaminant. The details of the approaches and the examination of the data are summarised below. Further details are provided by Fraser and Snelder (2019).

A2 Load calculation methods

A2.1 L7 model

Two regression model approaches to defining rating curves of (Cohn *et al.*, 1989, 1992) and (Cohn, 2005) are commonly used to calculate loads. The regression models relate the log of concentration to the sum of three explanatory variables: discharge, time, and season. The L7 model is based on seven fitted parameters given by:

$$\ln(\hat{C}_i) = \beta_1 + \beta_2 \left[\ln(q_i) - \overline{\ln(q)} \right] + \beta_3 \left[\ln(q_i) - \overline{\ln(q)} \right]^2 + \beta_4(t_i - \bar{T}) + \beta_5(t_i - \bar{T})^2 + \beta_6 \sin(2\pi t_i) + \beta_7 \cos(2\pi t_i) \quad (\text{Equation 2})$$

where, i is the index for the concentration observations, $\beta_{1,2,\dots,7}$: regression coefficients, t_i : time in decimal years, \bar{T} : mean value of time in decimal years, $\overline{\ln(q)}$ mean of the natural log of discharge on the sampled days, and \hat{C}_i : is the estimated i^{th} concentration.

The coefficients are estimated from the sample data by linear regression, and when the resulting fitted model is significant ($p < 0.05$), it is then used to estimate the concentration on each day in the sample period, $\ln(\hat{C}_j)$. The resulting estimates of $\ln(\hat{C}_j)$ are back-transformed (by exponentiation) to concentration units. Because the models are fitted to the log transformed concentrations the back-transformed predictions were corrected for retransformation bias. We used the smearing estimate (Duan, 1983) as a correction factor (S):

$$S = \frac{1}{n} \sum_{i=1}^n e^{\hat{\varepsilon}_i} \quad (\text{Equation 3})$$

where, $\hat{\varepsilon}$ are the residuals of the regression models, and n is the number of flow-concentration observations. The smearing estimate assumes that the residuals are homoscedastic and therefore the correction factor is applicable over the full range of the predictions.

The average annual load is then calculated by combining the flow and estimated concentration time series:

$$L = \frac{KS}{N} \sum_{j=1}^N \hat{C}_j Q_j \quad (\text{Equation 4})$$

If the fitted model is not significant, \hat{C}_j is replaced by the mean concentration and S is unity.

To provide an estimate of the load at a specific date, (i.e. $t^{\text{est}} = 1/3/2004$) a transformation is performed so that the year components of all dates (t_j) are shifted such that all transformed dates lie within a one-year period centred on the proposed observation date (i.e. $Y=1/9/2003$ to $31/8/2004$). For example, flow at time $t=13/6/2007$ would have a new date of $Y=13/6/2004$, and a flow at time $t=12/11/1998$ would have a new date of $Y=12/11/2003$.

$$\ln(\hat{C}_j^Y) = \beta_1 + \beta_2 \left[\ln(q_j) - \overline{\ln(q)} \right] + \beta_3 \left[\ln(q_j) - \overline{\ln(q)} \right]^2 + \beta_4(Y_j - \bar{T}) + \beta_5(Y_j - \bar{T})^2 + \beta_6 \sin(2\pi Y_j) + \beta_7 \cos(2\pi Y_j) \quad (\text{Equation 5})$$

where \hat{C}_j^Y is the estimated j^{th} concentration for the estimation year, and Y_j is the transformed date of the j^{th} observation, and all other variables are as per equation 6. We use this approach to estimate loads for the analysis that are representative of the middle of the state time period (i.e. the full calendar year of 2015). The regression coefficients ($\beta_{1,2,\dots,7}$) are those derived from fitting Equation 5 to the observation dataset. It follows that the estimated load for the year of interest can be calculated by:

$$L^Y = \frac{KS}{N} \sum_{j=1}^N \hat{C}_j^Y Q_j \quad (\text{Equation 6})$$

A2.2 L5 model

The L5 model is the same as L7 model except that two quadratic terms are eliminated:

$$\ln(\hat{C}_i) = \beta_1 + \beta_2(\ln(q_i)) + \beta_3(t_i) + \beta_4\sin(2\pi t_i) + \beta_5\cos(2\pi t_i) \quad (\text{Equation 7})$$

The five parameters are estimated, and loads are calculated in the same manner as the L7 model. Following the approach outlined for the L7 model, the L5 model can be adjusted when used for prediction to provide estimates for a selected load estimation date:

$$\ln(\hat{C}_j^Y) = \beta_1 + \beta_2[\ln(q_j)] + \beta_4(Y_j - \bar{T}) + \beta_6\sin(2\pi Y_j) + \beta_7\cos(2\pi Y_j) \quad (\text{Equation 8})$$

A2.3 Flow stratification

Roygard *et al.* (2012) employed a flow stratification approach to defining rating curves. This approach is based on a non-parametric rating curve, which is defined by evaluating the mean concentration within equal increments of the flow probability distribution (flow 'bins'). In their application, Roygard *et al.* (2012) employed ten equal time-based categories (flow decile bins), defined using flow distribution statistics and then calculated mean concentrations within each bin. This non-parametric rating curve can then be used to estimate nutrient concentrations, \hat{C} , for all days with flow observations. At step 2, the load is calculated following Equation 9, providing an estimate of average annual load over the observation time period.

$$L = \frac{K}{N} \sum_{j=1}^N \hat{C}_j Q_j \quad (\text{Equation 9})$$

where \hat{C}_j is calculated mean concentration associated with the flow quantile bin of the flow Q_j , and all other variables are as per equation 5.

A2.4 Flow stratification with trend

We included a modified version of the flow stratification method to account for trends in water quality. This is useful when loads are required to be estimated for a particular point in time, rather than as an average over the complete observation period, particularly when there is a strong trend evident. We detrended the observation data by fitting Equation 10 to the concentration time series.

$$\ln(\hat{C}_i) = \beta_1 + \beta_2(t_i) \quad (\text{Equation 10})$$

We then used the concentration residuals to develop a non-parametric rating curve. \hat{C}_j is calculated as the mean residual concentration associated with the flow quantile bin of the flow Q_j , plus the predicted value of concentration at time T_j , which is multiplied by the smearing coefficient to account for the log transformation of Equation 10).

A3 Precision of load estimates

The statistical precision of a sample statistic, in this study the mean annual load, is the amount by which it can be expected to fluctuate from the population parameter it is estimating due to sample error. In this study, the precision represents the repeatability of the estimated load if it was re-estimated using the same method under the same conditions. Precision is characterised by the standard deviation of the sample statistic, commonly referred to as the standard error. We evaluated the standard error of each load estimate by bootstrap resampling (Efron, 1981). For each load estimate we constructed 100 resamples of the concentration data (of equal size to the observed dataset), each of which was obtained by random sampling with

replacement from the original dataset. Using each of these datasets, we recalculated the site load and estimated the 95% confidence intervals, using the boot r package. We represent precision in the results as the 95% confidence interval range, standardised by the load estimate (i.e., represented as a proportion).

A4 Selection of best load estimation methodology

TN loads were calculated for all sites using each of the four load estimation methods. We evaluated the performance of each rating curve method for predicting observed concentrations, using a range of model performance measures (see Fraser and Snelder (2019) for details). We identified site loads and method combinations that had any of:

1. large export coefficient values (i.e., site load divided by catchment area);
2. large differences in the loads calculated using different methods.

For these site and method combinations (approximately 10-20% of sites for each nutrient variable), we manually inspected diagnostic plots (e.g., C-Q plots, C-T plots, comparisons of sampled flow distributions relative to observed flow distributions). We used expert judgement to select the most appropriate load estimation method for each site that were outside of the two criteria outlined above. As well as selecting from one of the four rating curve methods described above, we also allowed sites to be discarded at this stage if no method appeared to satisfactorily describe the observed behaviour. This process also suggested that, for the manually inspected sites, the selection of the model with the lowest RMSD (in terms of performance in predicting observed concentrations) was the criteria most consistent with the outcomes of the expert judgement. For the remainder of the site and nutrient variable combinations that were not flagged by the above criteria (and for which the diagnostic plots were not inspected), the most appropriate load estimation method was selected as the rating curve method that yielded the lowest RMSD.

Appendix B Analysis of Observed TP Loads and Sediment P Simulations at Water Quality Monitoring Sites

Relevant to this study is the recognition that the observed TP loads at the water quality monitoring sites are uncertain and, in fact, are likely under-estimates of the actual total instream TP loads. Under-estimation is likely because monitoring is based on punctual monthly sampling that poorly characterises TP concentrations under infrequent high-flow conditions. This is illustrated by Figure B-1, which shows the available monthly TP concentration observations for four sites in the Region plotted against the flow at the time of the observation. The plot indicates that concentration observations are predominantly at flows around the median, are rarely at flows as high as the mean annual flood flow, and there is an absence of data at the highest flows. The uncertainty of the observed TP loads arises because the monthly samples are used to construct a statistical model that predicts the loads on days without concentration observations (Snelder *et al.*, 2017).

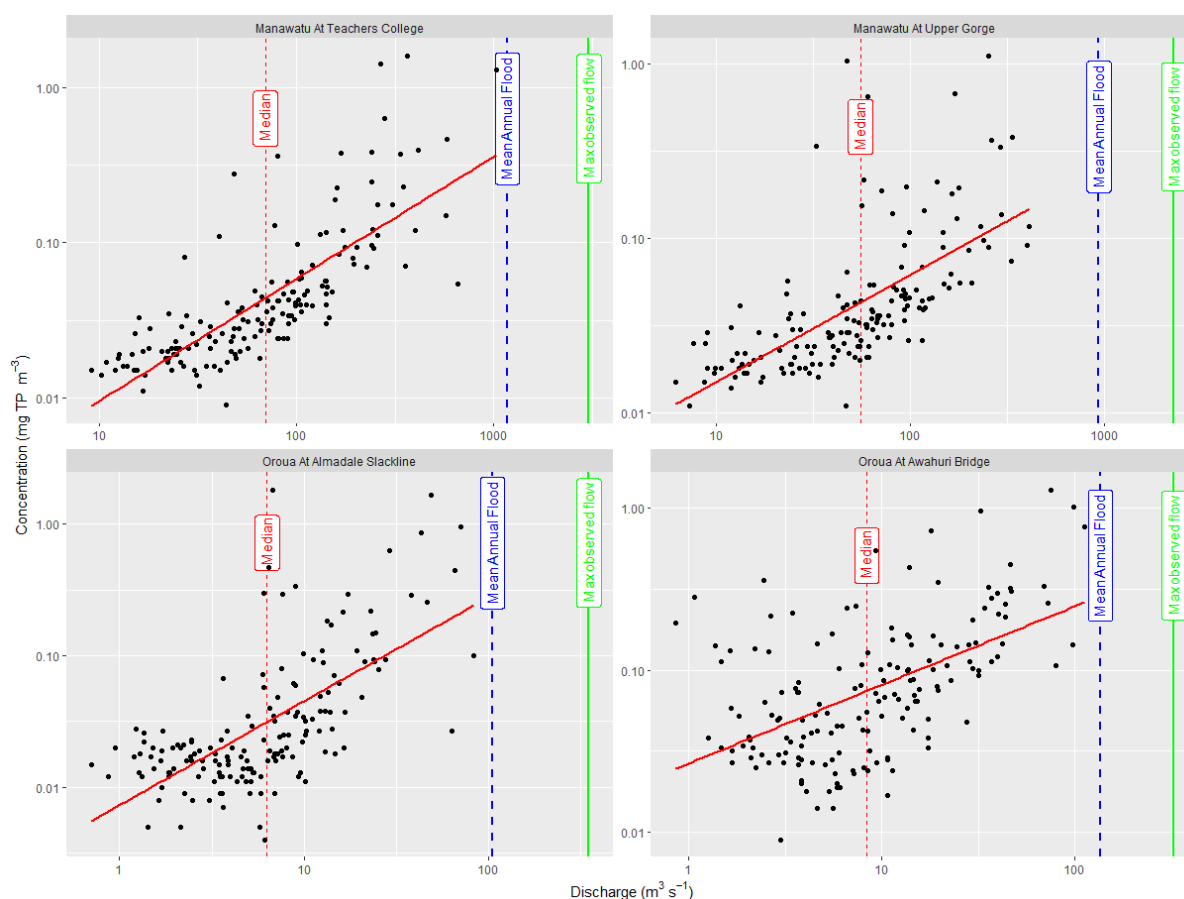


Figure B-1. Examples of monthly TP concentration observations for four water quality monitoring sites in the region plotted against the flow at the time of the observation. The black points indicate the concentration observations and the red solid line indicates a regression relationship fitted to the log (base 10) transformed concentration and flow. The red, blue and green vertical lines in each panel indicate the median, mean annual flood and maximum observed flow at each site.

Evidence that the calculated TP loads under-estimate the total TP load was derived using independent estimates provided by Vale *et al.* (2021). Vale *et al.* (2021) estimated TP loads

for every segment of the national digital river network in the Manawatū region using the SedNetNZ sediment model. SedNetNZ is a steady-state sediment budget model designed to represent the diversity of erosion processes that occur in the New Zealand landscape and predict mean annual suspended sediment yields (Dymond *et al.*, 2016). SedNetNZ represents individual sediment processes, including landslide, gully, and earthflow erosion, surficial erosion, bank erosion, and flood-plain deposition. SedNetNZ routes sediment contributions down catchments so that the total sediment yield at any location in the river network can be estimated. Importantly, SedNetNZ represents sediment generation and transport during extreme erosion events (i.e., major storms that cause erosion to occur on up to a decadal timescale).

Vale *et al.* (2022) converted sediment loads estimated by SedNetNZ (kg yr^{-1}) to equivalent TP loads based on observations of TP concentrations in suspended sediment in the Manawatū River at Teachers' College of 545 mg kg^{-1} made by Parfitt *et al.* (2013). We obtained the TP loads estimated using SedNetNZ from data supplied by Vale *et al.* (2022) for the locations of the 55 water quality monitoring sites in the Region. We converted these TP loads to equivalent yields (hereafter SedNetNZ TP yield) by dividing by the catchment area upstream of each water quality site ($\text{kg ha}^{-1} \text{ yr}^{-1}$).

We compared the SedNetNZ TP yield to the observed TP yield (by dividing the load calculated from the monthly samples as described in Section 2.3 by the upstream catchment area). The overall difference between the two sets of yields was characterised by the mean of the differences between estimates for each water quality monitoring site. Consistent with our expectations, the observed TP yields calculated by this study were, on average, 45% lower than the SedNetNZ TP yields (Figure B-2). We assume the primary reason for the differences between the observed and SedNetNZ TP loads is that the observed loads are missing at least a component of the total sediment erosion phosphorus (SEP) load, as defined in the body of this document.

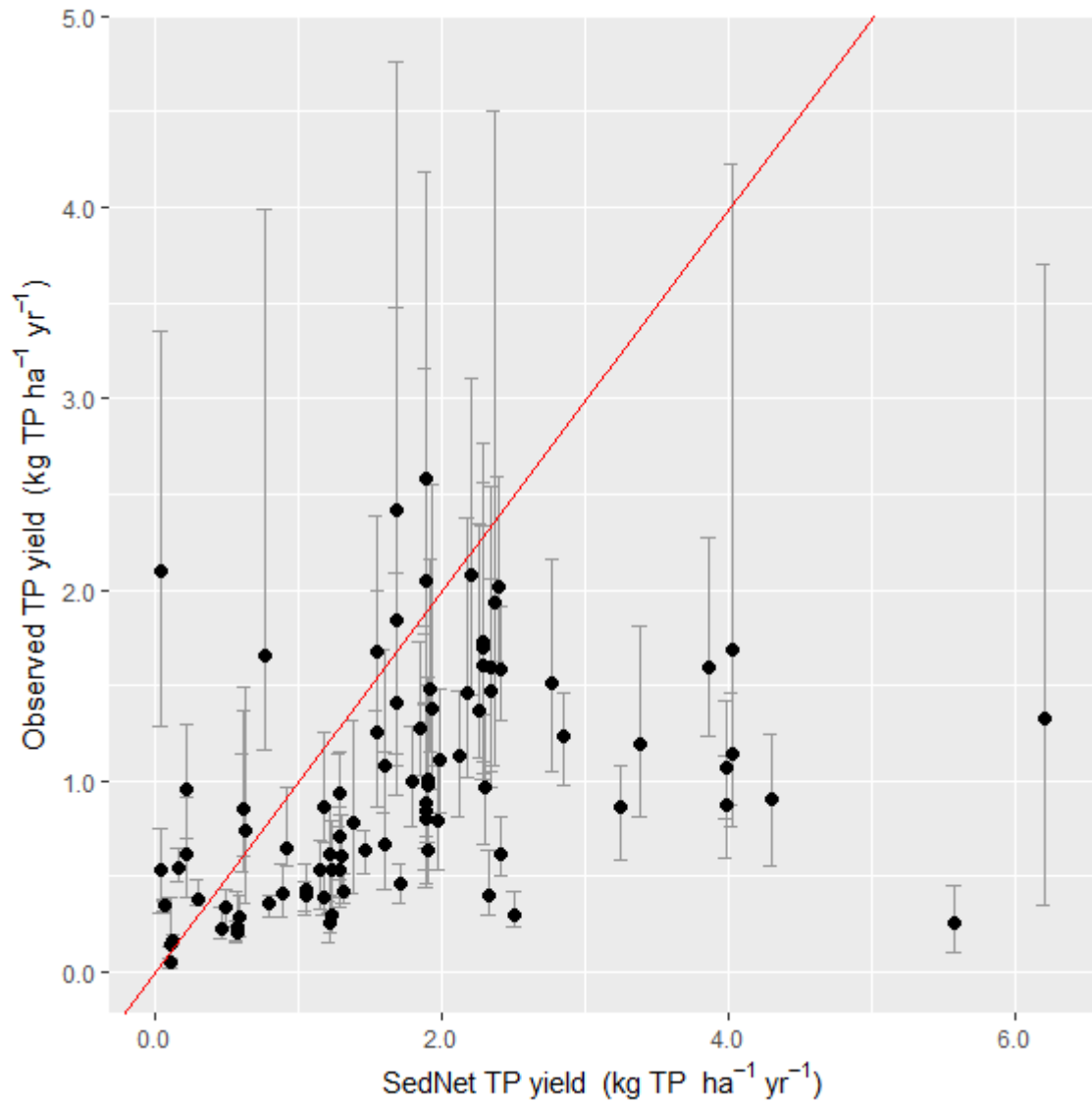


Figure B-2. Comparison of observed TP loads (expressed as yields) calculated for water quality monitoring sites by this study from monthly samples with yields calculated from sediment loads estimates made using SedNetNZ. The red line indicates perfect agreement (i.e., one to one).



horizons
REGIONAL COUNCIL



horizons.govt.nz

24 hour freephone 0508 800 800
fax 06 952 2929 | **email** help@horizons.govt.nz
Private Bag 11025, Manawatu Mail Centre, Palmerston North 4442